Journal of Experimental Botany Advance Access published May 27, 2014

Journal of Experimental Botany
doi:10.1093/jxb/eru191

Journal of Experimental Botany
www.jxb.oxfordjournals.org

DARWIN REVIEW

Linking chlorophyll *a* fluorescence to photosynthesis for remote sensing applications: mechanisms and challenges

Albert Porcar-Castell[1,*], Esa Tyystjärvi[2], Jon Atherton[1], Christiaan van der Tol[3], Jaume Flexas[4], Erhard E. Pfündel[5], Jose Moreno[6], Christian Frankenberg[7] and Joseph A. Berry[8]

[1] Department of Forest Sciences, University of Helsinki, PO Box 27, 00014 Helsinki, Finland
[2] Molecular Plant Biology, Department of Biochemistry, University of Turku, FI-20014 Turku, Finland
[3] Faculty of ITC, University of Twente, PO Box 217, 7524 AE Enschede, The Netherlands
[4] Plant Biology under Mediterranean Conditions, Universitat de les Illes Balears, Ctra. de Valldemossa Km. 7.5, 07122 Palma, Spain
[5] Heinz Walz GmbH, Eichenring 6, D-91090 Effeltrich, Germany
[6] Department of Earth Physics and Thermodynamics, Faculty of Physics, University of Valencia, C/ Dr. Moliner, 50, 46100 Burjassot, Valencia, Spain
[7] Jet Propulsion Laboratory, California Institute of Technology, Pasadena, CA 91109, USA
[8] Department of Global Ecology, Carnegie Institution of Washington, Stanford, CA 94305, USA

* To whom correspondence should be addressed. E-mail: joan.porcar@helsinki.fi

Received 14 February 2014; Revised 21 March 2014; Accepted 31 March 2014

Abstract

Chlorophyll *a* fluorescence (ChlF) has been used for decades to study the organization, functioning, and physiology of photosynthesis at the leaf and subcellular levels. ChlF is now measurable from remote sensing platforms. This provides a new optical means to track photosynthesis and gross primary productivity of terrestrial ecosystems. Importantly, the spatiotemporal and methodological context of the new applications is dramatically different compared with most of the available ChlF literature, which raises a number of important considerations. Although we have a good mechanistic understanding of the processes that control the ChlF signal over the short term, the seasonal link between ChlF and photosynthesis remains obscure. Additionally, while the current understanding of *in vivo* ChlF is based on pulse amplitude-modulated (PAM) measurements, remote sensing applications are based on

Abbreviations: A_G, gross photosynthetic rate (e.g. μmol CO_2 fixed by the Calvin–Benson cycle m^{-2} s^{-1}); A_N, net photosynthetic rate (e.g. μmol CO_2 exchanged at the leaf scale m^{-2} s^{-1}); APAR, the flux of photosynthetically active radiation absorbed by plants (e.g. μmol photons m^{-2} s^{-1}); a_I, a_{II}, relative absorption cross-section areas of PSI and PSII populations; range from zero to one; CET, cyclic electron transport; ChlF, chlorophyll *a* fluorescence; ETR, electron transport rate through PSII (μmol electrons m^{-2} s^{-1}), equivalent to LET; *F*, fluorescence signal emanating from a leaf, as in Equation 11; *f*APAR, fraction of incoming PAR absorbed by vegetation; range from zero to one; F_{II}, F_{IIM}, prevailing and maximal fluorescence signal at the level of PSII, respectively; $F_{PSI}(\lambda_{em})$,function that accounts for the shape of the fluorescence emission spectra in PSI; $F_{PSII}(\lambda_{em})$, function that accounts for the shape of the fluorescence emission spectra in PSII; F_R, F_{FR}, fluorescence measured in the red or far-red region, respectively; F', F_M', prevailing and maximal fluorescence signal as measured with PAM fluorometry (relative units, e.g. sensor mV output); F_0, F_M, minimal and maximal fluorescence signal as measured with PAM fluorometry in the dark and after a period of dark acclimation (relative units, e.g. sensor mV output); Φ*F*, quantum yield of fluorescence (quanta emitted/quanta absorbed); ΦF_I, ΦF_{II}, quantum yield of fluorescence in PSI and PSII, respectively; Φ*P*, quantum yield of photochemistry in PSII (electrons transported/quanta absorbed); ΦP_{max}, maximum quantum yield of photochemistry in PSII obtained after dark acclimation or during the night; GPP, gross primary productivity (e.g. total μmol CO_2 assimilated by plants m^{-2} s^{-1}); k_{CII}, rate constant of excitation energy transfer between neighbouring PSII units that denotes the degree of excitonic connectivity (s^{-1}); k_D, rate constant of basal or constitutive thermal energy dissipation (s^{-1}); k_F, rate constant of chlorophyll fluorescence emission (s^{-1}); k_{ISC}, rate constant of intersystem crossing (s^{-1}); k_{NPQ}, rate constant of regulated thermal energy dissipation or NPQ (s^{-1}); k_P, overall rate constant of photochemistry (s^{-1}); k_{PSII}, intrinsic rate constant of photochemistry in open and fully functional reaction centres (s^{-1}); k_{RCI}, rate constant of thermal energy dissipation by closed PSI (s^{-1}); k_T, rate constant of energy transfer between neighbouring pigments (s^{-1}); LET, linear electron transport; LUE, light use efficiency of photosynthesis (μmol CO_2 assimilated/quanta absorbed); NPQ, non-photochemical quenching of excitation energy via regulated thermal energy dissipation; *NPQ* (in italics), a fluorescence parameter to quantify NPQ capacity, proportional to $k_{NPQ}/(k_D+k_F)$; PQ, photochemical quenching of excitation energy via electron transport; *PQ* (in italics), a fluorescence parameter to quantify PQ capacity, proportional to $k_P/(k_D+k_F)$; PR, photorespiration rate (μmol CO_2 photorespired m^{-2} s^{-1}); PRI, photochemical reflectance index; PSI, photosystem I; PSII, photosystem II; *q*, fraction of open and functional reaction centres; range from zero to one. *q*L, the photochemical quenching parameter based on a lake model assumption, an estimate of *q*; *q*P, the photochemical quenching parameter based on a puddle model assumption, an estimate of *q*; R_d, the rate of leaf-level mitochondrial day respiration (e.g. μmol CO_2 respired m^{-2} s^{-1}); SIF, solar-induced fluorescence (e.g. in W m^{-2} s^{-1} nm^{-1} s^{-1}), also sun-induced fluorescence.

the measurement of the passive solar-induced chlorophyll fluorescence (SIF), which entails important differences and new challenges that remain to be solved. In this review we introduce and revisit the physical, physiological, and methodological factors that control the leaf-level ChlF signal in the context of the new remote sensing applications. Specifically, we present the basis of photosynthetic acclimation and its optical signals, we introduce the physical and physiological basis of ChlF from the molecular to the leaf level and beyond, and we introduce and compare PAM and SIF methodology. Finally, we evaluate and identify the challenges that still remain to be answered in order to consolidate our mechanistic understanding of the remotely sensed SIF signal.

Key words: Gross primary production, GPP, leaf level, photosystem II, photosystem I, PSII, PSI, photosynthesis dynamics, pulse amplitude modulation, PAM, PSII connectivity, remote sensing, solar-induced fluorescence, sun-induced fluorescence, SIF.

1. Introduction

Photosynthesis drives the global carbon cycle. Net photosynthesis can be quantified at the leaf level by monitoring CO_2 exchange using chamber enclosure systems combined with infrared gas analysers (Long and Bernacchi, 2003), and at the ecosystem level using flux towers and eddy covariance techniques (Goulden *et al.*, 1996; Baldocchi, 2008). At the landscape and regional levels, gross photosynthetic CO_2 assimilation, or gross primary productivity (GPP), is inferred using models and algorithms that integrate ground observations with remotely sensed data (e.g. Heinsch *et al.*, 2006; Williams *et al.*, 2009; Jung *et al.*, 2011). Remotely sensed data have been extensively used to infer GPP based on the light use efficiency (LUE) model (Moneith, 1972; Kumar and Moneith, 1981; Zhao *et al.*, 2011). In the LUE model, GPP is proportional to incoming photosynthetically active radiation (PAR), the fraction absorbed by vegetation (*f*APAR), and the LUE at which absorbed radiation is used by photosynthesis:

$$\mathrm{GPP} = \mathrm{PAR}\ f\mathrm{APAR}\ \mathrm{LUE} \quad (1)$$

Remote sensing has been traditionally used to estimate the first two terms of this equation (see reviews by Hilker *et al.*, 2008; Malenovsky *et al.*, 2009). For example, differences in surface reflectance between the red, blue, and near infrared part of the spectrum have been exploited to derive a wide range of vegetation indices to assess *f*APAR, green biomass, chlorophyll content, or leaf area index (e.g. Rouse *et al.*, 1974; Huete, 1988; Qi *et al.*, 1994; Huete *et al.*, 1997; Daughtry *et al.*, 2000; Haboudane *et al.*, 2002). Typically, vegetation indices show a strong seasonal correlation with GPP in many plant communities (e.g. grasslands, croplands, and deciduous forests), but the correlation breaks down in evergreen plant communities where seasonal changes in GPP are strongly modulated by LUE as well as *f*APAR (Equation 1) (e.g. Sims *et al.*, 2006; Garbulsky *et al.*, 2008). To represent the dynamics of LUE, remote sensing data have been used to classify vegetation into plant functional types (PFTs). Subsequently, global GPP models combine spatially resolved PFT and other remote sensing products [e.g. PAR, *f*APAR, temperature, and vapour pressure deficit (VPD)] with functions and parameters derived from flux tower observations to estimate LUE (Heinsch *et al.*, 2006; Williams *et al.*, 2009; Jung *et al.*, 2011).

Although the LUE approach provides a theoretical basis for constructing and calibrating models, there are no corresponding benchmarks to evaluate model performance at large geographical scales, and model uncertainty remains high (Beer *et al.*, 2010). The situation could be dramatically improved if a new source of data was available that captured the dynamic behaviour of photosynthesis at the relevant scale. Fortunately, photosynthesis generates an optical signal that, in addition to PAR and *f*APAR, is also sensitive to LUE. This signal is chlorophyll *a* fluorescence (ChlF). ChlF are photons of red and far-red light that are emitted by chlorophyll *a* pigments nanoseconds after light absorption. Because photosynthesis and ChlF compete for the same excitation energy, ChlF carries information on LUE.

ChlF has been used for decades to elucidate the organization, function, and acclimation of the photosynthetic apparatus at the subcellular and leaf levels (see seminal reviews by Krause and Weis, 1991; Govindjee, 1995; Lázar, 1999; Maxwell and Johnson, 2000; Baker, 2008). Originally restricted to the laboratory, ChlF measurements made their move to the field with the development of the pulse amplitude-modulated (PAM) technique (an active technique that involves the use of a measuring light and a saturating light pulse), and the subsequent introduction of commercial PAM fluorometers (Schreiber *et al.*, 1986; Bolhàr-Nordenkampf *et al.*, 1989). PAM fluorometry has facilitated the study of the acclimation of photosynthesis *in situ* and helped clarify the link between ChlF and photosynthetic CO_2 assimilation. Yet, despite the importance and value of PAM fluorometry, for practical reasons the technique has been restricted to the leaf level, and its applicability at the canopy and landscape levels remains unknown. To fill the gap, the field of ChlF has recently seen a new wave of developments that seek to measure ChlF from remote sensing platforms.

The remote sensing technique is based on the passive measurement of solar-induced chlorophyll fluorescence (SIF). The goal is to use the seasonal dynamics in the SIF signal measured from towers, aircrafts, and satellites as a proxy of photosynthesis (Grace *et al.*, 2007; Hilker *et al.*, 2008; Meroni *et al.*, 2009; Rascher *et al.*, 2009). During the last decade, SIF has been successfully measured from tower (Moya *et al.*, 2004; Rossini *et al.*, 2010; Guanter *et al.*, 2013; Drolet *et al.*, 2014), aircraft (Zarco-Tejada *et al.*, 2009, 2012, 2013), and satellite platforms (Guanter *et al.*, 2007; Joiner *et al.*, 2011; Frankenberg *et al.*, 2011; Guanter *et al.*, 2012), the

latter yielding the first global maps of terrestrial ChlF from GOSAT, SCIAMACHY, and GOME-2 (Frankenberg *et al.*, 2011; Joiner *et al.*, 2011, 2013). New space missions, which are in the later stages of development (e.g. NASA OCO-2, GOSAT-2, and ESA Sentinels 4–5), will provide better coverage of SIF data and open up new study possibilities, by using sensors primarily designed to monitor atmospheric chemistry. In turn, the FLEX mission (Moreno *et al.*, 2006), in the latest stage of evaluation by the European Space Agency (ESA), has been specifically designed and optimized to map ChlF at a spatial resolution of 300 m, providing high resolution and global coverage. The amount, quality, and spatiotemporal coverage of SIF data are rapidly increasing. However, we are left with important questions. Are we ready to exploit all the information carried by the SIF signal? Can we export the knowledge obtained from short-term PAM studies to decipher the seasonal dynamics in SIF?

Remote sensing of ChlF takes place at a different spatiotemporal domain and uses a different methodology compared with the majority of ChlF studies in the literature. Amongst others, PAM fluorescence is measured over a broad spectral region whereas SIF is estimated within very narrow spectral bands. PAM fluorescence is not affected by ambient illumination whereas the SIF signal is. Most importantly of all, while we have a good mechanistic understanding of the processes that control the ChlF signal over the short term (from seconds to days), the interplay between the seasonal acclimation of photosynthesis and the ChlF signal remains unknown. Clearly, there is an urgent need to compile and re-examine the underlying theory in the context of the new applications, to identify the open questions, and to establish a roadmap that encourages the needed breakthroughs.

The goal of this review is to introduce and revisit the physical, physiological, and methodological factors that control the ChlF signal in the context of remote sensing applications, and to identify those research questions that remain open. This review is also conceived as a general introduction of ChlF for the broad community involved in the remote sensing of ChlF.

For simplicity, we focus on the leaf level because it is the smallest spatial scale at which fluorescence and photosynthetic CO_2 uptake can be mechanistically linked and measured simultaneously. Up-scaling the signal from the leaf to the scales observed by airborne or spaceborne sensors falls in the domain of canopy–atmosphere radiative transfer, something equally essential to interpret SIF but outside the scope of the present review.

The review is organized in four main sections. In Section 2, we present the basis of photosynthesis and its optical signals to clarify the potential and limitations of optical data, and to introduce the multitude of processes that are embedded in Equation 1. In Section 3 we introduce the biophysical and physiological basis of ChlF from the molecular level to the leaf level and beyond, providing the theoretical and mechanistic knowledge needed to understand the spatiotemporal dynamics of the ChlF signal from the context of remote sensing. In Section 4 we introduce and compare PAM and SIF fluorometry, clarifying the main differences. Finally, in Section 5 we identify and discuss the challenges that remain to be solved, proposing further experimental work. Alternatively, the reader may wish to skip the background theory presented in Sections 2 and 3 and come back to if later on for reference.

2. The regulation of photosynthesis and its optical signals

Photosynthesis involves two main sets of reactions: the light reactions, where electromagnetic energy is absorbed by pigments and converted into chemical energy in the form of ATP and NADPH; and the carbon fixation reactions, where ATP and NADPH are used to produce sugars from atmospheric carbon dioxide. Because the light and carbon reactions exhibit different sensitivities to environmental variables such as light, temperature, or water availability, the production of ATP and NADPH by the light reactions and consumption of these metabolites by the carbon reactions do not always match (Ögren *et al.*, 1984; Huner *et al.*, 1996; Ensminger *et al.*, 2006).

Energy absorbed in excess by the light reactions can damage the photosynthetic machinery (Barber and Andersson, 1992; Demmig-Adams and Adams, 2000; Tyystjärvi, 2013), for example a leaf in a sunny (high energy input) but cold (low energy consumption) environment. Accordingly, plants have evolved a number of regulatory mechanisms to adjust the energy balance between the light and carbon reactions (Walters, 2005; Demmig-Adams and Adams, 2006). The result of this continuous adjustment is that the performance of the light reactions of photosynthesis (visible to optical sensors) tends to emulate that of the carbon reactions. This establishes a link between optical data and GPP that can be implemented to the remote sensing of photosynthesis. Some processes, however, interfere with the relationship, which we discuss below (Fig. 1).

2.1 Light absorption and its regulation

Photosynthesis starts with absorption of light, mainly by chlorophyll molecules. Accordingly, an effective mechanism used by plants to regulate light absorption, or *f*APAR, consists of adjusting the concentration of chlorophyll pigments in the leaf (Fig. 1). The relationship between chlorophyll content and light absorption is non-linear because the increment in light absorption per unit of chlorophyll decreases at high chlorophyll contents (Adams *et al.*, 1990; Gitelson *et al.*, 1998). Net changes in leaf-level chlorophyll are visible over time scales of days (García-Plazaola and Becerril, 2001; Lu *et al.*, 2001). In addition, certain plant species use other mechanisms to modulate photosynthetic light absorption that operate at different temporal scales: leaf movements and leaf angle adjustments (Yu and Berg, 1994; Arena *et al.*, 2008), chloroplast movements (Brugnoli and Björkman, 1992; Sarvikas *et al.*, 2010), changes in surface reflectance mediated by salt bladders (Mooney *et al.*, 1977; Esteban *et al.*, 2013), changes in leaf epicuticular wax properties (Pfündel et al., 2006; Olascoaga *et al.*, 2014), changes in leaf

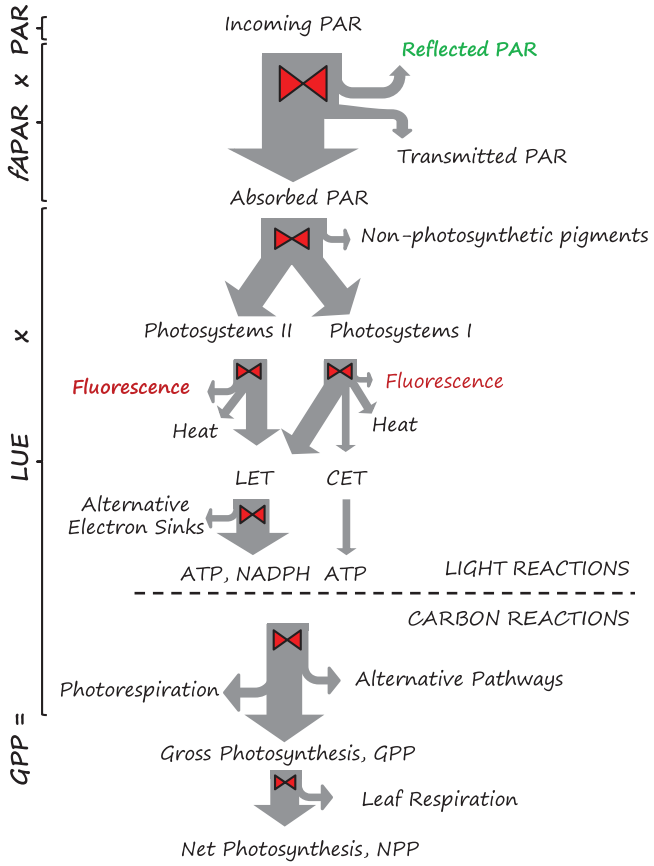

Fig. 1. Photosynthetic energy partitioning at the leaf level and the light use efficiency model (GPP=PAR *f*APAR LUE). Red valve symbols indicate the action of regulatory mechanisms which adjust the energy partitioning between pathways (grey arrows). Grey arrows represent the flow of energy. Optical signals available to remote sensing include properties of reflected light (shown in green) and chlorophyll *a* fluorescence (shown in red). LET, linear electron transport; CET, cyclic electron transport.

surface structures such as pubescence (Ehleringer *et al.*, 1976; Morales *et al.*, 2002; Galmés *et al.*, 2007*a*), and changes in the concentration of non-photosynthetic pigments such as anthocyanins (Close and Beadle, 2003; Pfündel et al., 2006; Merzlyak *et al.*, 2008) (Fig. 1). The temporal dynamics of these processes need to be considered when interpreting ChlF data because changes in light absorption have a direct impact on ChlF intensity (see Section 3). A special case is that of non-photosynthetic pigments which do not contribute to ChlF or photosynthesis, but increase leaf absorptance (Hlavinka *et al.*, 2013).

2.2 Linear and cyclic electron transport and energy distribution between photosystems

Photosynthetic pigments are bound by proteins to form photosynthetic antenna complexes (Liu *et al.*, 2004) that capture light energy and transfer it to a reaction centre. A reaction centre is a special pigment–protein complex that converts excitation energy to chemical energy. The combination of reaction centre and antenna is termed a photosystem. Higher plants have two types of photosystems: photosystem I (PSI) and photosystem II (PSII), which actually operate in series in the opposite order, that is with electrons being transferred from PSII to PSI (Fig. 2).

After a photon is captured by a chlorophyll molecule in PSII, the excitation energy rapidly reaches the reaction centre chlorophyll, referred to as P680 (a pigment with absorption maximum at 680 nm). Excited P680* rapidly gives an electron to the primary electron acceptor, pheophytin, which in turn reduces the quinone A (Q_A) electron acceptor to yield the first stable charge-separated state $P680^+Q_A^-$. Subsequently, Q_A^- passes an electron to quinone B (Q_B) which leaves its binding site when double reduced and protonated by stromal protons.

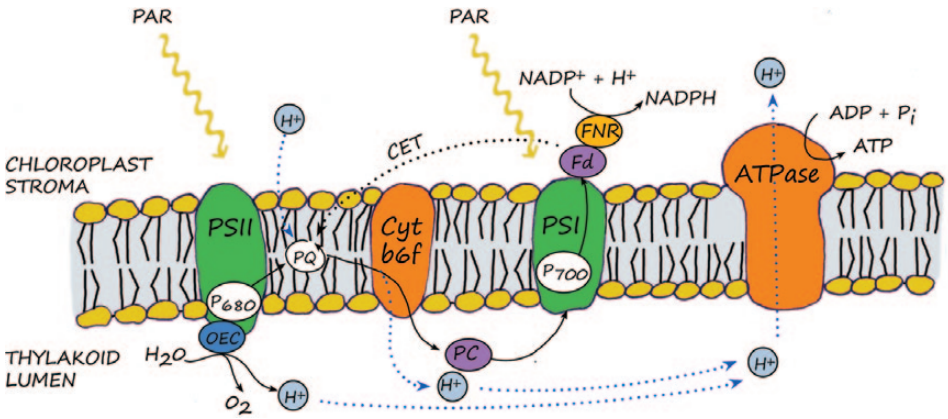

Fig. 2. Schematic representation of the photosynthetic linear electron transport (LET) chain. In LET, excitation energy from absorbed photons in PSII is used to reduce the plastoquinone pool ('PQ') and pump protons from the chloroplast stroma into the thylakoid lumen via the Cyt b_6f complex. Energy from absorbed photons in PSII is also used to operate the oxygen-evolving complex (OEC) by which water molecules are split yielding further protons. Simultaneously, the energy from photons absorbed by PSI is used, via ferrodoxin (Fd), by ferrodoxin-NADPH reductase (FNR) to reduce $NADP^+$ to NADPH. The oxidized PSI reaction centre $P700^+$ is reduced back to P700 using an electron donated by plastocyanin (PC), originally from PSII. In cyclic electron transport (CET), an electron is passed from Fd back to the PQ pool and again to PSI via PC. This results in pumping of protons to the lumen but no NADPH synthesis. Protons accumulated in the lumen (from either LET or CET) are used by ATP synthase (ATPase) to synthesize ATP.

Protonated Q_B reduces plastoquinone ('PQ', not to be confounded with photochemical quenching PQ), which is subsequently reoxidized by the cytochrome b_6f complex (Cyt b_6f), eventually transferring the protons to the thylakoid lumen (Fig. 2). At the donor side, $P680^+$ is reduced by tyrosine Z (TyrZ); subsequently $TyrZ^+$ takes up an electron from the oxygen-evolving complex (OEC) which is responsible for the splitting of the water molecule and the release of oxygen and protons (Antal *et al.*, 2013). The resulting protons, together with those pumped to the lumen by the Cyt b_6f complex, accumulate in the thylakoid lumen, generating a proton concentration gradient across the thylakoid membrane (Kramer *et al.*, 2004*a*). This gradient is used by ATP synthase (ATPase) to synthesize ATP. Simultaneously, energy absorbed in PSI is captured by its reaction centre chlorophyll (P700) and used to reduce the electron acceptor ferrodoxin (Fd). Oxidized $P700^+$ is reduced back to P700 by taking an electron from plastocyanin (PC). From ferredoxin, the electron is passed to $NADP^+$ to produce NADPH in a reaction catalysed by ferrodoxin-NADPH reductase (FNR). This series of reactions makes up the linear electron transport (LET) (for reviews, see Ort and Yocum, 1996; Antal *et al.*, 2013).

Efficient operation of the LET implies that the populations of PSII and PSI work in series and their reaction centres transfer electrons at approximately similar rates. Although a trivial solution would be to allocate the same relative antenna cross-section area to PSII and PSI, extra flexibility is required. For example, the absorption spectra of PSII and PSI are different due to differences in pigment composition and spectral forms (see Section 3.2), with PSI absorbing light of slightly longer wavelengths (Duysens and Sweers, 1963; Boichenko, 1998; Pfündel, 2009). In particular, PSI has a higher proportion of chlorophyll *a* compared with PSII, with chlorophyll *a*/*b* ratios of 9 for PSI compared with 2.5 for PSII, in extracted photosystem particles (Ben-Shem *et al.*, 2003; Nield and Barber, 2006). As a result, the probabilities of light absorption by PSII and PSI will change depending on the spectral properties of incoming light, and its temporal and spatial dynamics.

Another factor that calls for extra flexibility in energy partitioning between photosystems is the operation and dynamics of cyclic electron transport (CET) (Joliot and Joliot, 2002; Rumeau *et al.*, 2007). CET translocates electrons around PSI and pumps protons from the chloroplast stroma to the thylakoid lumen (Fig. 2). Because the electron is recycled, CET yields only ATP but no NADPH. Functionally, CET is thought to contribute to the efficient induction of the Calvin–Benson cycle upon illumination of dark-acclimated leaves (Joliot and Joliot, 2002), the regulation of the lumen pH, and thereby modulation of non-photochemical quenching in the photosystems, NPQ (see below) (Kramer *et al.*, 2004*a*), or the protection of PSI against photoinhibition (Rumeau *et al.*, 2007; Sonoike, 2011). Indeed, CET has been found to be essential for normal carbon fixation in many C_4 plants (Hatch, 1992). To summarize, changes in light quality and CET require flexible mechanisms capable of adjusting the energy partitioning between PSII and PSI (i.e. the relative absorption cross-sections of PSII and PSI, a_{II} and a_I, respectively) (Fig. 1).

At a time scale of minutes, the partitioning of energy between photosystems (a_{II} and a_I) is regulated through a process known as state transitions (Murata, 1969; Haldrup *et al.*, 2001; Tikkanen *et al.*, 2011). Under low light, if leaves are illuminated with light that favours PSII, part of the peripheral antenna complexes of PSII can migrate to serve PSI. This has the effect of balancing the energy input between the photosystems. State transitions are considered to be important only under low light conditions (Rintamäki *et al.*, 1997; Haldrup *et al.*, 2001; Tikkanen *et al.*, 2011), and are therefore of little relevance for remote sensing.

At time scales of days, photosystem stoichiometry and a_{II} and a_I can adjust in response to more sustained changes in light intensity and quality (Anderson *et al.*, 1988; Chow *et al.*, 1990; Durnford and Falkowski, 1997; Pfannschmidt *et al.*, 1999; Haldrup *et al.*, 2001). Light intensity and quality co-vary within a plant canopy, with shaded parts of the canopy or understorey plants receiving light enriched in far-red due to absorption of red light by foliage above. The result is that leaves in shaded environments tend to display higher a_{II}:a_I ratios than more exposed foliage (Anderson *et al.*, 1988; Chow *et al.*, 1990; Rivadossi *et al.*, 1999; Hihara and Sonoike, 2001; Eichelmann *et al.*, 2005; Ballotari et al., 2007). In addition to their functional and energetic role, the spatiotemporal dynamics of a_{II} and a_I have important implications for the interpretation of ChlF because they affect the shape of the fluorescence spectra and the magnitude of the PSI fluorescence contribution (Palombi *et al.*, 2011), as well as the estimation of the LET rate by means of fluorescence (see Section 4.1).

Evidence suggests that CET and energy partitioning between photosystems might be highly dynamic in response to stress and environmental conditions (Martin *et al.*, 1978; Ivanov *et al.*, 2001; Eichelmann *et al.*, 2005; Rumeau *et al.*, 2007). However, the seasonal and spatiotemporal dynamics of these traits remain poorly understood.

2.3 Energy partitioning at the photosystem level

Understanding the processes that control the energy partitioning in PSII is crucial to linking ChlF with photosynthetic CO_2 assimilation. Energy absorbed by pigments of PSII is dissipated by three main pathways: (i) it can be used by photochemistry (by LET); (ii) it can be dissipated non-radiatively as heat; or (iii) it can be re-emitted as a photon of fluorescence. A unique relationship between ChlF and photochemical efficiency cannot be established. This is because non-radiative dissipation of excitation energy is dynamic and under physiological control (see Section 3).

In low light and in the absence of stress, most of the absorbed energy is effectively used by photochemistry, and the excitation lifetime in the antenna of PSII (τ_{PSII}) is short (in the order of hundreds of picoseconds) (Dau, 1994; Lavergne and Trissl, 1995; Gilmore *et al.*, 1995). This results in lowered fluorescence yield. This de-excitation pathway is termed photochemical quenching (PQ) (a term originally coined to denote the quenching of the fluorescence signal but herein used to address the photochemical quenching of excitation

energy). If light intensity increases, the carbon fixation reactions and electron transport chain gradually become light saturated, causing an increase in τ_{PSII}. This results in increased fluorescence yield. The sudden increase in fluorescence yield, observed when subjecting a dark-acclimated leaf to strong illumination, and the subsequent decrease are collectively referred as the Kautsky effect (e.g. Govindjee, 1995). These rapid fluorescence dynamics reflect the rapid reduction and re-oxidation of PSII electron acceptors and their influence on τ_{PSII} (see Section 3.2) (Brody and Rabinovitch, 1957).

Plants are incentivized to keep τ_{PSII} as low as possible, while still permitting photochemical trapping. This acts to minimize the formation of chlorophyll triplet states which might lead to production of singlet oxygen, a hazardous reactive oxygen species (Barber and Andersson, 1992). As a result, plants have evolved a number of regulatory mechanisms that are capable of dissipating the excess quanta as heat (see reviews by Müller *et al.*, 2001; Demmig-Adams and Adams, 2006; Garcia-Plazaola *et al.*, 2012). The operation of these mechanisms results in a decrease in the excitation lifetime in the antenna and subsequently a decrease in the ChlF yield. This type of de-excitation pathway is commonly referred to as non-photochemical quenching (NPQ), after being widely estimated using the fluorescence parameter *NPQ* (Bilger and Björkman, 1991) (see Section 4.1). However, it should be kept in mind that the regulated thermal dissipation of excitation energy (non-photochemical quenching of excitation energy) and the parameter *NPQ* (non-photochemical quenching of the fluorescence signal) are not always equivalent; thus, it becomes practical to separate NPQ and *NPQ* (Porcar-Castell 2011; García-Plazaola *et al.*, 2012). For example, when state transitions reduce the PSII relative absorption cross-section (a_{II}), the fluorescence signal is lowered (and the *NPQ* parameter increases) because fewer photons are absorbed by PSII (Horton and Hague, 1988), but no change takes place in τ_{PSII}. In the following, we use NPQ and *NPQ* accordingly.

The regulation of NPQ in PSII involves mechanisms operating at different time scales. In the short term (seconds to hours), two ΔpH-dependent mechanisms appear to regulate thermal energy dissipation in PSII (Müller *et al.*, 2001; Demmig-Adams and Adams, 2006; Garcia-Plazaola *et al.*, 2012). When the electron transport chain saturates, proton accumulation tends to decrease lumen pH (Fig. 2). Subsequently, the PsbS protein acts as a proton sensor activating and de-activating NPQ, while lumen pH regulates the activity of the enzyme violaxanthin de-epoxidase (VDE). The lowering of the pH triggers the de-epoxidation of violaxanthin to zeaxanthin, resulting in amplified NPQ (Demmig-Adams, 1990; Horton *et al.*, 1996; Müller *et al.*, 2001; Jahns and Holzwarth, 2012). This second mechanism operates at time scales of minutes. Together, the protonation of antenna proteins and de-epoxidation of xanthophyll cycle pigments have been traditionally addressed as energy-dependent quenching (qE) (Weis and Berry, 1987; Krause and Weis, 1991; Horton *et al.*, 1996). Recently, another zeaxanthin-dependent (qZ) but ΔpH-independent form of NPQ was found in *Arabidopsis* and suggested also to operate at a time scale of minutes (Nilkens *et al.*, 2010). All these mechanisms modulate NPQ over the course of the day in response to diurnal fluctuations in light and temperature. These NPQ forms relax in the dark (e.g. overnight) and are accordingly termed flexible or reversible NPQ (Müller *et al.* 2001; Demmig-Adams *et al.*, 2006; Porcar-Castell, 2011).

Over longer time scales (days to weeks) plants face more sustained changes in their environment (e.g. drought or low winter temperatures). At the seasonal scale, the light-harvesting machinery undergoes sustained changes that result in down-regulation of the photochemical quenching capacity (PQ) and up-regulation of the non-photochemical quenching capacity (NPQ) in PSII (Ottander *et al.*, 1991, 1995; Verhoeven *et al.*, 1996; Ensminger *et al.*, 2004; Porcar-Castell *et al.*, 2008*a*; Porcar-Castell, 2011). These adjustments are termed sustained because they do not recover overnight. The decrease in PQ is associated with the accumulation of damaged/photoinhibited PSII reaction centres. Damage and recovery of reaction centres take place simultaneously (Kok, 1956; Ohad *et al.*, 1984; Greer *et al.*, 1986). Thus photoinhibition becomes apparent when damage occurs faster than recovery and, since the rate constant of photoinhibition is proportional to incoming light intensity (Tyystjärvi and Aro, 1996) while the rate of recovery is temperature dependent (Greer *et al.*, 1986), photoinhibition becomes apparent under strong light and particularly when strong light is combined with low temperatures (Strand and Lundmark, 1987; Ottander *et al.*, 1991; Campbell and Tyystjärvi, 2012; Tyystjärvi, 2013). The term photoinhibition has also been used to denote a decrease in the maximum quantum yield of photochemistry, commonly estimated via the fluorescence parameter F_V/F_M (see Section 4.1). The seasonal decrease in F_V/F_M or 'photoinhibition' has been shown to be caused by reaction centre damage, the presence of sustained NPQ, or a combination of both (Porcar-Castell *et al.*, 2008*b*). In this review, we use the term photoinhibition to refer to the damage of the reaction centre exclusively.

The increase in sustained NPQ has been associated with the overnight retention of a de-epoxidized xanthophyll cycle, the accumulation of the PsbS protein, the aggregation of light-harvesting complexes (LHCs) (Adams and Demmig-Adams, 1994; Ottander *et al.*, 1995; Verhoeven *et al.*, 1996; Ensminger *et al.*, 2004; Zarter *et al.*, 2006), as well as with changes in the redox properties of the electron acceptors of PSII that promote thermal dissipation in the reaction centre (Krause, 1988; Ivanov *et al.*, 2002, 2008; Matsubara and Chow, 2004); see Verhoeven (2014) for a recent review on sustained forms of NPQ. While the correlation between NPQ (i.e. thermal energy dissipation) and the parameter *NPQ* (i.e. fluorescence signal quenching) is well understood over the diurnal scale, the correlation between NPQ and *NPQ* at the seasonal scale remains obscure (Porcar-Castell, 2011), which in turn complicates the interpretation of seasonal time series of ChlF data.

In contrast to PSII, the lifetime of excitation in PSI (τ_{PSI}) does not seem to be affected by photochemical and non-photochemical quenching processes (at least over the short term) possibly because its reaction centre is very efficient in quenching excitation energy in the oxidized state. The result is a relatively low and constant contribution of fluorescence from

PSI to the total signal (Genty *et al.*, 1990*b*; Pfündel, 1998; Palombi *et al.*, 2011) that can be treated as a constant signal offset (e.g. Porcar-Castell *et al.*, 2006). However, the seasonal dynamics of PSI ChlF remain unknown.

In addition to ChlF, the regulation in energy partitioning at PSII generates another optical signal. The operation of the xanthophyll cycle and the fast regulation of NPQ in PSII are associated with changes in reflectance at ~531 nm (Gamon *et al.*, 1990). This feature is exploited by the photochemical reflectance index (PRI) (Gamon *et al.*, 1992), an index that has been shown to track changes in LUE through its correlation with NPQ (Evain *et al.*, 2004; Nichol *et al.*, 2006). The potential of the PRI as a remote sensing proxy of LUE has been demonstrated (Drolet *et al.*, 2005; Garbulsky *et al.*, 2008). However, the PRI has also been shown to be very sensitive to canopy structure, gap fraction, background, viewing angle, or leaf area index (Barton and North, 2001; Sims *et al.*, 2006; Goerner *et al.*, 2011), complicating the association of PRI and LUE. In addition, although the short-term variation in leaf-level PRI appears indeed to be controlled by NPQ, the seasonal variation in leaf-level PRI seems to be controlled by the slow changes in pigment pools rather than NPQ (Stylinski *et al.*, 2002; Filella *et al.*, 2009; Porcar-Castell *et al.*, 2012). The mechanistic link between the PRI and LUE appears to be highly dependent on scale and remains to be fully elucidated.

2.4 Alternative electron transport sinks and metabolic pathways

ChlF can be used to estimate the rate of LET through PSII (see Section 4.1). However, a number of processes need to be taken into account if we are to infer the rate of gross photosynthetic CO_2 assimilation or the rates of ATP and NADPH production from fluorometric estimates of LET. Because CET produces ATP but no NADPH, fluorometrically estimated LET will decouple from ATP production in the presence of CET (Fig. 1). Additionally, alternative electron transport sinks such as chlororespiration (Nixon, 2000) and the Mehler reaction (Asada, 2000) reduce the overall quantum yield of NADPH, further decoupling LET from NADPH production.

Alternative electron sinks are generally assumed to be small relative to LET, although they play an important functional role and can become significant under certain conditions. For example, the rate of chlororespiration has been shown to increase under high light and high temperature (Diaz *et al.*, 2007) and suggested to contribute to excess energy dissipation in the alpine plant *Ranunculus glacialis* (Laureau *et al.*, 2013). The Mehler reaction, in turn, has been shown to be stimulated under some water stress conditions (Biehler and Fock, 1996; Flexas *et al.*, 1999; Asada 2000). In addition, part of ATP and NADPH produced by the light reactions can be used by alternative metabolic pathways (e.g. nitrate and sulphate reduction in chloroplasts, or emission of plant volatile organic compounds) (Fig. 1). Krivosheeva *et al.* (1996) found that the electron transport rate and photosynthetic CO_2 uptake were decoupled in overwintering Scots pine, suggesting an increase in an alternative electron sink or metabolic pathway. Overall, the action of alternative sinks and metabolic pathways may, under certain conditions, affect the ability of ChlF to track the dynamics of photosynthetic CO_2 assimilation.

2.5 Carboxylation, oxygenation, and day respiration

The ATP and NADPH generated by the light reactions are utilized by the Calvin–Benson cycle to synthesize sugars by assimilating CO_2 (gross photosynthetic assimilation or A_G) (Fig. 1). Net photosynthetic assimilation (A_N) is the quantity that is measurable by gas exchange systems and relates to 'true' or gross photosynthesis (A_G) as:

$$A_N = A_G - PR - R_d \quad (2)$$

where R_d is the rate of mitochondrial day respiration and PR is the rate of photorespiration (Ogren, 1984). In photorespiration, Rubisco catalyses the oxidation (adding O_2) instead of the carboxylation (adding CO_2) of ribulose bisphosphate, with the oxidized product being partially recovered via the emission of CO_2. Because fluorometrically estimated LET (see Section 4.1) relates to A_G rather than A_N, the magnitude of photorespiration and mitochondrial respiration needs to be taken into account when comparing gas exchange and ChlF measurements.

In C_4 plants (e.g. maize and sorghum), photorespiration is almost fully suppressed, and fluorometrically estimated LET correlates well with net photosynthesis (e.g. Genty *et al.*, 1990*a*; Krall and Edwards, 1992). In C_3 plants, which include practically all tree species and the majority of higher plants, the energy flow going to photorespiration is considerable and variable. Flexas and Medrano (2002) showed that for a pool of different species the quantum yield of photorespiration increased in response to mild water stress, from 18% to 22%, while the quantum yield of photochemistry stayed approximately constant. Thus, processes such as photorespiration may undermine the capacity of ChlF to track plant stress under certain conditions.

The temperature sensitivity of mitochondrial respiration may vary seasonally, diurnally, or within a plant, in response to variations in maintenance respiration (Atkin *et al.*, 2005). For example, R_d has been found to increase from 15% of A_N to as much as 50% in response to drought stress (Flexas et al., 2005; Galmés *et al.*, 2007*b*), and a similar temporal pattern has been observed in boreal Scots pine foliage, with higher R_d values during spring recovery of photosynthesis compared with summer (Kolari *et al.*, 2007). In summary, CET, alternative electron sinks, photorespiration, and mitochondrial respiration can all decouple optical data such as ChlF from net photosynthetic CO_2 assimilation.

3. Physical and physiological controls of chlorophyll *a* fluorescence across space and time

In this section we describe how the intensity, spectrum, and dynamics of the ChlF signal *in vivo* are controlled by a number of scale-dependent physical and physiological factors (including photosynthesis).

Fluorescence is radiative loss of the energy of absorbed photons. Because part of the energy of the absorbed photon is lost as heat, the energy of the emitted photon is usually lower (longer wavelength) than that of the absorbed photon, a phenomenon known as Stokes shift. The quantum yield of fluorescence emission depends on both the properties of the fluorescing chromophore and its surroundings. Chlorophylls in ether are highly fluorescent, with quantum yields of 30% and 15% for chlorophyll *a* and chlorophyll *b*, respectively (Latimer *et al.*, 1956; Barber *et al.*, 1989). Carotenoids, in turn, yield very little fluorescence (Gillbro and Cogdell, 1989). In contrast, the quantum yield of ChlF *in vivo* does not exceed 10%, with typical values under steady-state illumination of 0.5–3% (Latimer *et al.*, 1956; Brody and Rabinovitch, 1957; Krause and Weis, 1991). This drastic decrease is due to the photochemical and non-photochemical quenching of excitation energy in the photosynthetic antennae, making ChlF such a valuable tool for assessing photosynthesis.

3.1 Chlorophyll fluorescence at the molecular level

Energy levels of atomic and molecular orbitals are quantized, but molecules present wide, continuous absorption and emission (fluorescence) spectra because vibrational energies of the molecule are superimposed on each electronic energy level. A photon can be absorbed if its energy equals the difference in the sum of electronic, vibrational, and rotational energies between an excited-state orbital and the ground-state orbital. Vibrational energy is vibration of atoms about their equilibrium positions in the molecule. Because photosynthetic pigments *in vivo* are tightly packed into a protein matrix, the vibration of the chemical bonds in the pigment–protein complex add additional variability to the absorption and emission spectra of pigments *in vivo*. This phenomenon, known as inhomogeneous broadening, explains why photosynthetic pigments display different spectral forms *in vivo* (Vassiliev and Bruce, 2008) but not when isolated. Rotational energy is associated with the rotation of the molecule around its axis, which is negligible in the solid state.

In Fig. 3 we portray an idealized representation of the energy levels and possible energy dissipation pathways for a chlorophyll *a* molecule embedded in a photosynthetic antenna. Chlorophyll *a* absorbs photons of blue and red light very efficiently. Absorption of a blue photon raises an electron from the ground-state orbital (S_0) to an orbital of a high excited state. Part of the energy is transformed to molecular vibrations and rapidly dissipated (Jennings *et al.*, 2003). Subsequently, because vibrational energy levels from higher excited states overlap with those of the S_1 level, electrons originally in an orbital of a higher excited state can switch to

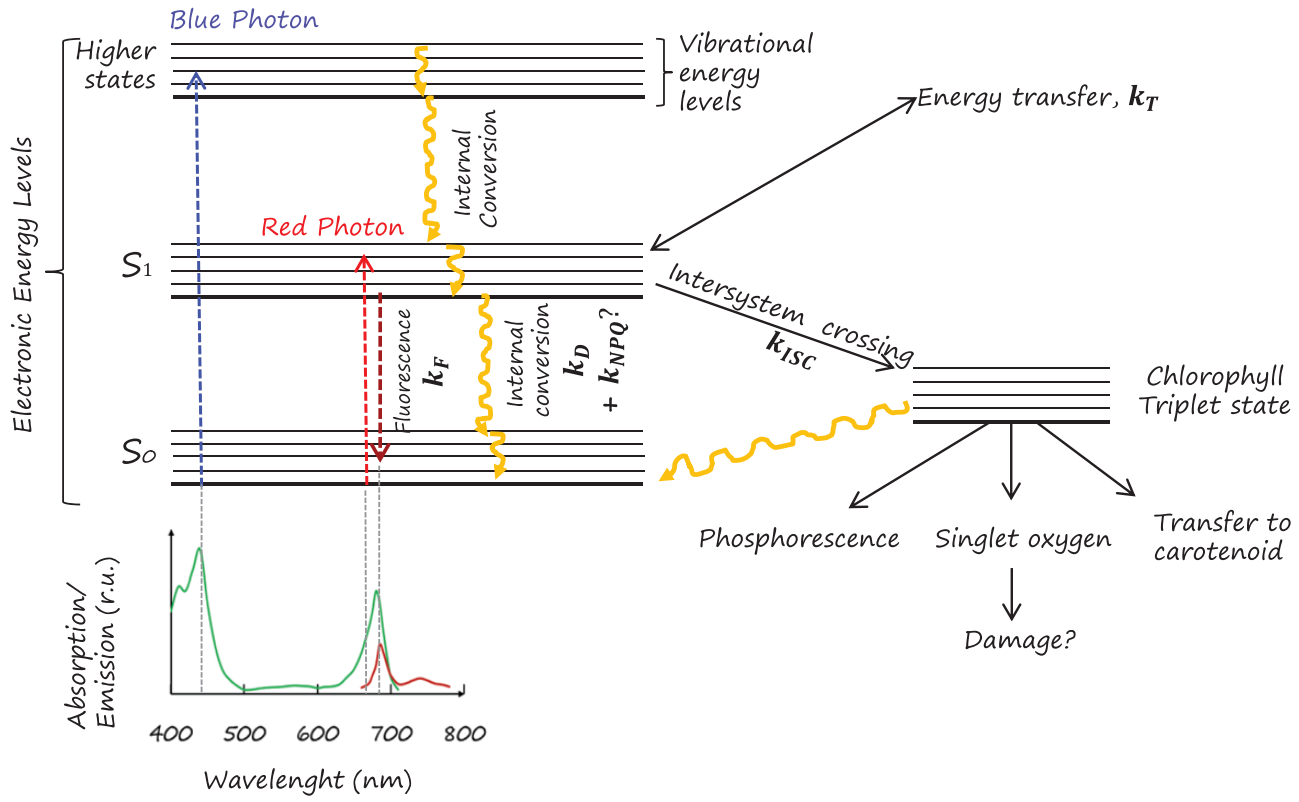

Fig. 3. Idealized Jablonski diagram illustrating the energy partitioning of absorbed photons in a chlorophyll *a* molecule. Upon absorption of a photon of blue light, an electron from the ground state is raised to a higher energy state. The energy is rapidly dissipated non-radiatively as heat mainly by internal conversion, and the electron rapidly relaxes to the first excited state (S_1). In contrast, absorption of a red photon produces the S_1 state directly. It is from S_1 that photosynthetic energy partitioning starts. The electron can relax to the ground state via emission of a chlorophyll fluorescence photon (with an associated rate constant k_F), via non-radiative thermal dissipation, by means of either constitutive (k_D) or physiologically regulated mechanisms (k_{NPQ}), via energy transfer to another pigment or to the reaction centre chlorophyll (k_T), or via intersystem crossing to form a chlorophyll triplet state (k_{ISC}). In turn, triplet states can be deactivated via phosphorescence, reaction with oxygen to form singlet oxygen, or by transfer to a carotenoid.

the vibrational manifold of the S_1 level, and the vibrational energy is again rapidly dissipated. The phenomenon is called internal conversion and it populates the first excited state of a chlorophyll molecule in hundreds of femtoseconds to 10 picoseconds after absorption of a photon (Dau and Sauer, 1996; Jennings *et al.*, 2003; Clegg, 2004). A photon of red light produces the S_1 state directly. It is important to note that the difference in energy between a photon of red light and a photon of shorter wavelengths (higher energy) is virtually always dissipated as heat; for this reason, it is more practical to express photosynthetic efficiencies on a quantum rather than an energy basis.

Energy partitioning takes place from S_1. Excitations in the S_1 state live a thousand times longer compared with those in the higher energy states, and therefore other processes compete with internal conversion for dissipation of excitation from S_1 to S_0 (Fig. 3). In addition to internal conversion, the excitation energy can be transferred to another pigment. Excitation energy can also be lost via emission of a fluorescence photon. Furthermore, a change in the spin state can occur and produce a chlorophyll triplet state, a process called intersystem crossing (Clegg, 2004). The triplet state is long lived and relaxes either by reacting with oxygen to produce reactive singlet oxygen (Tyystjärvi, 2004), by transfer of energy to a carotenoid or other prenyllipid, by internal conversion to the ground state, or by emission of a phosphorescence photon (Hoff, 1986). Finally, the rate constant of thermal dissipation of S_1 states appears to be under physiological control at the photosystem level, at least in PSII. This regulated component of thermal dissipation corresponds to the NPQ mechanism described in Section 2.3. There is no consensus on whether NPQ is enhancement of internal conversion (e.g. by a mechanism that brings chlorophyll *a* molecules close to each other), enhancement of transfer of energy from chlorophyll *a* to zeaxanthin (followed by internal conversion producing the ground state of the carotenoid), or both (Owens *et al.*, 1992; Holt *et al.*, 2005; van Grondelle and Novoderezhkin, 2006). We choose to introduce NPQ already at the molecular level for consistency although NPQ would be meaningful at the level of photosystem. Macroscopically, constitutive or basal thermal dissipation (D) is defined as the minimum thermal dissipation rate obtained in the absence of stress and down-regulation. Any increase in thermal dissipation on top of that is attributed to NPQ.

The quantum efficiency of a process (*i*) that competes for excitation energy with *n* other processes, and where k_i is the first-order rate constant of the *i*th process, can be expressed as (Govindjee, 2004):

$$\Phi_i = \frac{k_i}{\sum_{i=0}^{i=n} k_i} \quad (3)$$

Accordingly, the quantum yield of fluorescence at the molecular level (Fig. 3) can be expressed as:

$$\Phi F_{\mathrm{Chl}a} = \frac{k_F}{k_D + k_F + k_{ISC} + k_{PB} + k_T(+k_{NPQ})} \quad (4)$$

where k_D is assumed to be the first-order rate constant associated with the process of internal conversion, k_F is the rate constant of fluorescence emission, k_{ISC} is the rate constant of intersystem crossing leading to chlorophyll triplet states, k_{PB} the rate constant of photobleaching or destruction of the chlorophyll molecule, k_T the rate constant of energy transfer to a neighbouring pigment molecule, and k_{NPQ} the rate constant of regulated thermal energy dissipation (NPQ). All reactions are of the first order and therefore the rate constants are expressed as 1/time unit (s^{-1}). The lifetime of excitation is the inverse of the sum of all rate constants ($\tau = 1/\Sigma k_i$). The rate constant of fluorescence (k_F) depends on the properties of the chlorophyll molecule and is assumed to remain constant in physiological processes (Butler and Kitajima, 1975; Clegg, 2004). The rate constant k_D is invariable by definition (i.e. any variation is embedded in k_{NPQ}). The rate constants k_{ISC} and k_{PB} are orders of magnitude smaller than k_D or k_F (Clegg, 2004; Santabarbara *et al.*, 2007) and, since they are not relevant for energy partitioning, we hereafter consider them as part of k_D. Finally, the rate constant of energy transfer between pigments k_T includes two main mechanisms: coherent energy transfer, and Förster or fluorescence resonance energy transfer (FRET) (Nedbal and Szöcs, 1986; Clegg, 2004; Engel *et al.*, 2007; Novoderzhkin and van Grondelle, 2010). In general, energy transfer between closely coupled pigments within a single antenna protein can be described as movement of delocalized excitons (coherent energy transfer), whereas energy transfer between pigment–protein complexes requires consideration of localized excited states (Förster energy transfer) (Novoderzhkin and van Grondelle, 2010).

3.2 Chlorophyll fluorescence at the photosystem and thylakoid membrane level

Interpreting ChlF dynamics at the level of thylakoid membrane requires the use of a number of assumptions the validity of which depends on the temporal context of the application. The assumptions listed below are generally accepted when interpreting slow ChlF dynamics (seconds to minutes), but they are too simplified to interpret fast fluorescence kinetics successfully (picosecond to second range) (e.g. Lazár, 1999; Zhu *et al.*, 2005; Stirbet, 2013). Similarly, some of the assumptions may be equally challenged at the seasonal scale, something that will be addressed in this section.

Assumption (A): single pool model. Photosynthetic antennae have evolved to collect photons and effectively deliver the energy to a reaction centre (Fig. 4). Efficient energy transfer from pigment to pigment and to the reaction centre is very rapid (time constants 10 fs to 10 ps) (Clegg, 2004; Engel *et al.*, 2007; Novoderzhkin and van Grondelle, 2010) in comparison with the 200–500 ps required for stable charge separation (Roelofs *et al.*, 1992; Vassiliev and Bruce, 2008). A large body of evidence supports the idea of rapid excitation equilibration in the antennae of PSII and PSI (Schatz *et al.*, 1988; Croce *et al.*, 1996; Dau and Sauer, 1996; Andrizhiyevskaya *et al.*, 2004; Miloslavina *et al.*, 2006). If we assume rapid excitation equilibration, the antenna, core, and reaction centre can be treated as a single pigment pool

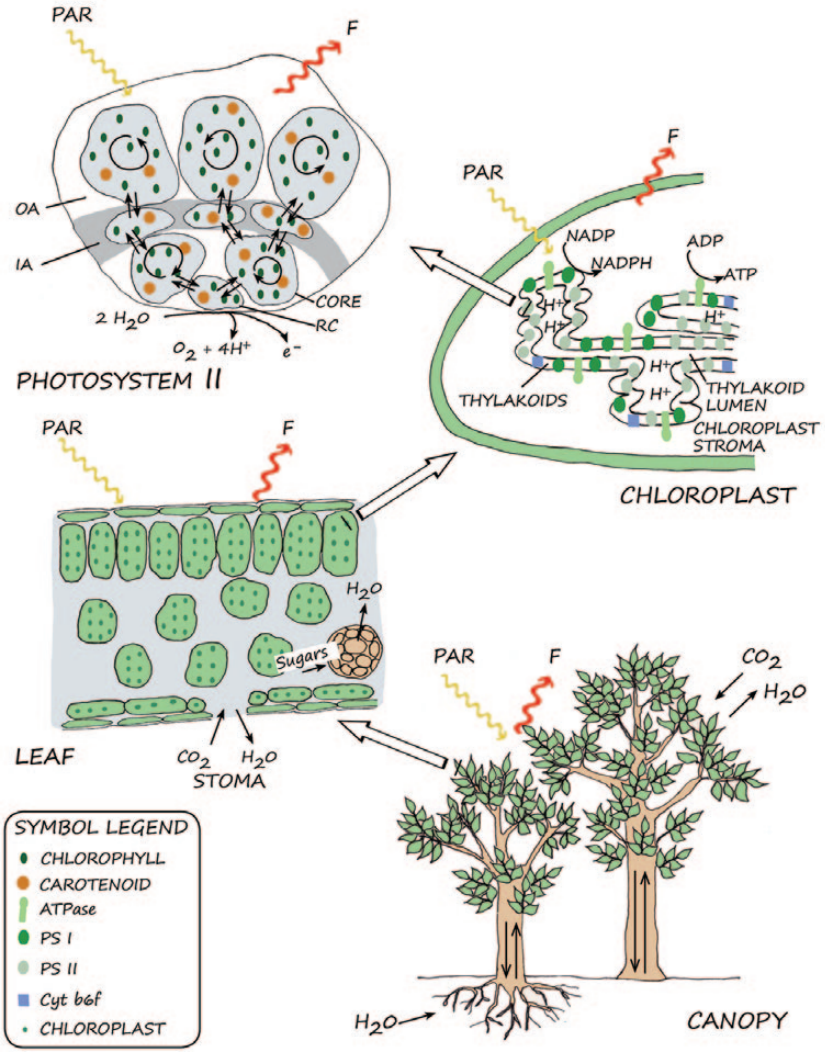

Fig. 4. Chlorophyll *a* fluorescence and photosynthesis from the photosystem to the canopy level. (A) At the photosystem level, excitation energy is transferred (black arrows) between pigments from the outer antenna (OA), inner antenna (IA), core, and reaction centre (RC) where it can be used to drive photochemistry. A variable part of this excitation energy is lost as heat or re-emitted as chlorophyll fluorescence (*F*). At the photosystem level, the quantum yield of fluorescence largely depends on the capacity of the above photochemical and non-photochemical processes, whereas the fluorescence spectral properties largely depend on chlorophyll–protein conformation and antenna structure. (B) At the chloroplast level, populations of photosystem II (PSII) and photosystem I (PSI) cooperate for light absorption and together contribute to the resulting fluorescence signal, with quantum yield and spectral properties differing between photosystems. (C) At the leaf level, cells and their chloroplasts are arranged to optimize light absorption within the leaf. This distribution results in important wavelength-dependent light gradients within the leaf and wavelength-dependent reabsorption of fluorescence. (D) At the canopy level, strong vertical gradients in light quality and intensity produce gradients in photosystem size, PSII:PSI stoichiometry, thylakoid organization, leaf morphology, and leaf pigment concentrations. The chlorophyll fluorescence signal and its relationship to photosynthesis increase in complexity with increasing scale.

(Dau, 1994; Lavergne and Trissl, 1995). This greatly simplifies the analysis of ChlF data (Fig. 4).

Assumption (B): no spillover. We consider that the populations of PSII and PSI are energetically isolated and that the rate of transfer of excitations from PSII to PSI (Kitajima and Butler, 1975*b*; Trissl and Wilhelm, 1993; Tan *et al.*, 1998), known as spillover, can be assumed to be insignificant at ambient temperature.

Assumption (C): no thermal dissipation by closed reaction centres. We consider that thermal energy dissipation by closed reaction centres (with $P680^+$) is only relevant when analysing ChlF data that have been excited using intense laser sources, in which the time elapsed between absorption of two consecutive photons by PSII is shorter than the lifetime of $P680^+$ (Shinkarev and Govindjee, 1993).

Assumption (D): no quenching by oxidized plastoquinone. Excitation quenching by oxidized plastoquinone is relatively small (Vernotte *et al.*, 1979), with a rate constant that reaches $0.15(k_f+k_D)$ when at its maximum (Zhu *et al.*, 2005) (i.e. equivalent to NPQ=0.15).

Assumption (E): perfect connectivity/lake model. The main link between ChlF dynamics and photosynthesis dynamics originates at the level of PSII, via the photochemical reaction. The photochemical reaction is defined as the stable charge separation including reduction of the Q_A electron acceptor and advancement of the Kok

cycle (Britt, 1996). Photochemistry can only take place in reaction centres that are open and functional (i.e. are associated with an oxidized Q_A and fully operational). We define the fraction of open and functional reaction centres q, which ranges from zero (when all reaction centres are closed) to one (when reaction centres are open and functional). Accordingly, ChlF will increase with decreasing q but the relationship depends on the degree to which excitation can move from closed to open PSII centres, a phenomenon known as connectivity (Joliot and Joliot, 1964; Havaux *et al.*, 1991; Lavergne and Trissl, 1995; Kramer *et al.*, 2004*b*) and recently reviewed by Stirbet (2013).

If k_{CII} is the rate constant of the excitation energy transfer between two connected PSII units (see Appendix 1), then three different types of connectivity models can be defined (Dau, 1994; Lavergne and Trissl, 1995; Stirbet, 2013): a separate units or puddle model, where $k_{CII}=0$; a lake model, where all photosystems share excitation from a single pool and $k_{CII}=\infty$; and models with finite connectivity ($0<k_{CII}<\infty$). Importantly, except for the special cases when $q=0$ (termed maximal fluorescence F_M), or when $q=1$ (termed minimal fluorescence F_0) (Kitajima and Butler, 1975*a*; Dau, 1994; Lavergne and Trissl, 1995), connectivity will interact with the relationship between ChlF and q. Accordingly, it is important to select a model that approximates the level of connectivity in the sample. Two extreme approaches have been used to estimate q: (i) the qP parameter (Schreiber *et al.*, 1986; van Kooten and Snel, 1990) based on a separate units model; and (ii) the qL parameter (Kramer *et al.*, 2004*b*; Baker, 2008; Porcar-Castell, 2011) based on a lake model, where qL=q for a system with perfect connectivity, and qP=q for a system with no connectivity at all (Appendix 1), with intermediate qL and qP performances depending on connectivity (see Fig. 5 and text below).

The bulk of experimental data favours the view that PSII units are connected to some extent (Joliot and Joliot, 1964; Dau et al., 1994; Lavergne and Trissl, 1995; Kramer *et al.*, 2004*b*; Tyystjärvi *et al.*, 2009) although some recent data favour a model of isolated centres (Oja and Laisk, 2012). Overall, the lake model has been described as a reasonable assumption to study the slow ChlF dynamics dealt with here (Kramer *et al.*, 2004*b*; Baker, 2008). These conclusions need to be re-assessed at the seasonal scale for three reasons: (i) The effect of connectivity (excitation transfer from closed to open centres) could expand to photoinhibited reaction centres (excitation transfer from damaged to functional centres); (ii) connectivity might undergo changes at the seasonal scale; and (iii) connectivity effects have been analysed in the absence of or under constant and relatively low levels of NPQ, but the interplay between connectivity and NPQ remains unknown.

Lavergne and Trissl (1995) derived equations for examining the impact of different connectivity models on fluorescence yield as a function of the fraction of open reaction centres (q). Applying those equations (Appendix 1), we evaluated the impact of NPQ on connectivity and the interplay between connectivity, NPQ, qL, and qP (Fig. 5). The analysis demonstrates that connectivity has very little effect on ChlF in the presence of NPQ (Fig. 5A–D). Therefore, the impact of connectivity on seasonal changes of ChlF obtained under natural illumination (as in the remote sensing of SIF) is probably small. In contrast, selecting a proper connectivity model remains important even in the presence of NPQ if q needs to be estimated. In a nutshell, overestimation of q by qP increases with connectivity, and underestimation of q by qL decreases with connectivity (Fig. 5E–L). If we use the lake model assumption to interpret ChlF data, a seasonal decrease in connectivity would translate into underestimation of q and consequently to underestimation of ΦP (Equation 9). A decrease in connectivity would also decrease the overall probability of photochemical excitation trapping by reaction centres. Accordingly, the effects of connectivity on ChlF and on the 'true' ΦP tend to cancel out (Weis and Berry, 1987), and therefore fluorometric estimates of ΦP are expected to be good proxies of 'true' ΦP irrespective of connectivity issues. Keeping this in mind, we use the lake model assumption and the parameter qL as a proxy of q to demonstrate the derivation of the quantum yield of photochemistry in PSII (see Section 4.1 for application to PAM fluorometry).

The effective rate constant of photochemistry (k_P) depends on the maximum intrinsic rate constant of photochemistry (k_{PSII}) proportionally to qL as:

$$k_P = qLk_{PSII} \tag{5}$$

Subsequently, the fluorescence flux of PSII (F_{II}) (µmol photons m^{-2} s^{-1}) emanating from a sample with area (m^{-2}) that contains a large population of both PSII and PSI units can be expressed as a function of the quantum yield of fluorescence emission (ΦF_{II}):

$$F_{II} = IAa_{II}\,\Phi F_{II} \tag{6}$$

where I is the incident flux of photosynthetic active radiation (µmol photons m^{-2} s^{-1}), A is the absorptance coefficient, and a_{II} the relative absorption cross-section area of the PSII population in the sample. Applying Equation 3, ΦF_{II} can be expressed as:

$$\Phi F_{II} = \frac{k_F}{k_D + k_F + k_{NPQ} + qLk_{PSII}} \tag{7}$$

Equations 6 and 7 introduce the link between ChlF and photochemistry at the level of PSII. It should be clarified that these equations (and the rate constants therein) are only meaningful when applied to large populations of photosystems. Because both k_{NPQ} and qL vary in response to the acclimation of photosynthesis, a direct link between ChlF and photochemistry cannot be readily established with Equation 7 alone. An additional fluorescence measurement in a different state is needed.

Estimation of the quantum yield of photochemistry of PSII (ΦP) is accomplished by measuring ChlF in the presence ($0<q<1$) and in the absence of photochemistry ($q=0$). This has been traditionally accomplished using herbicides such as DCMU (e.g. Horton and Hague, 1988), liquid nitrogen temperature (Björkman and Demmig, 1987), and more

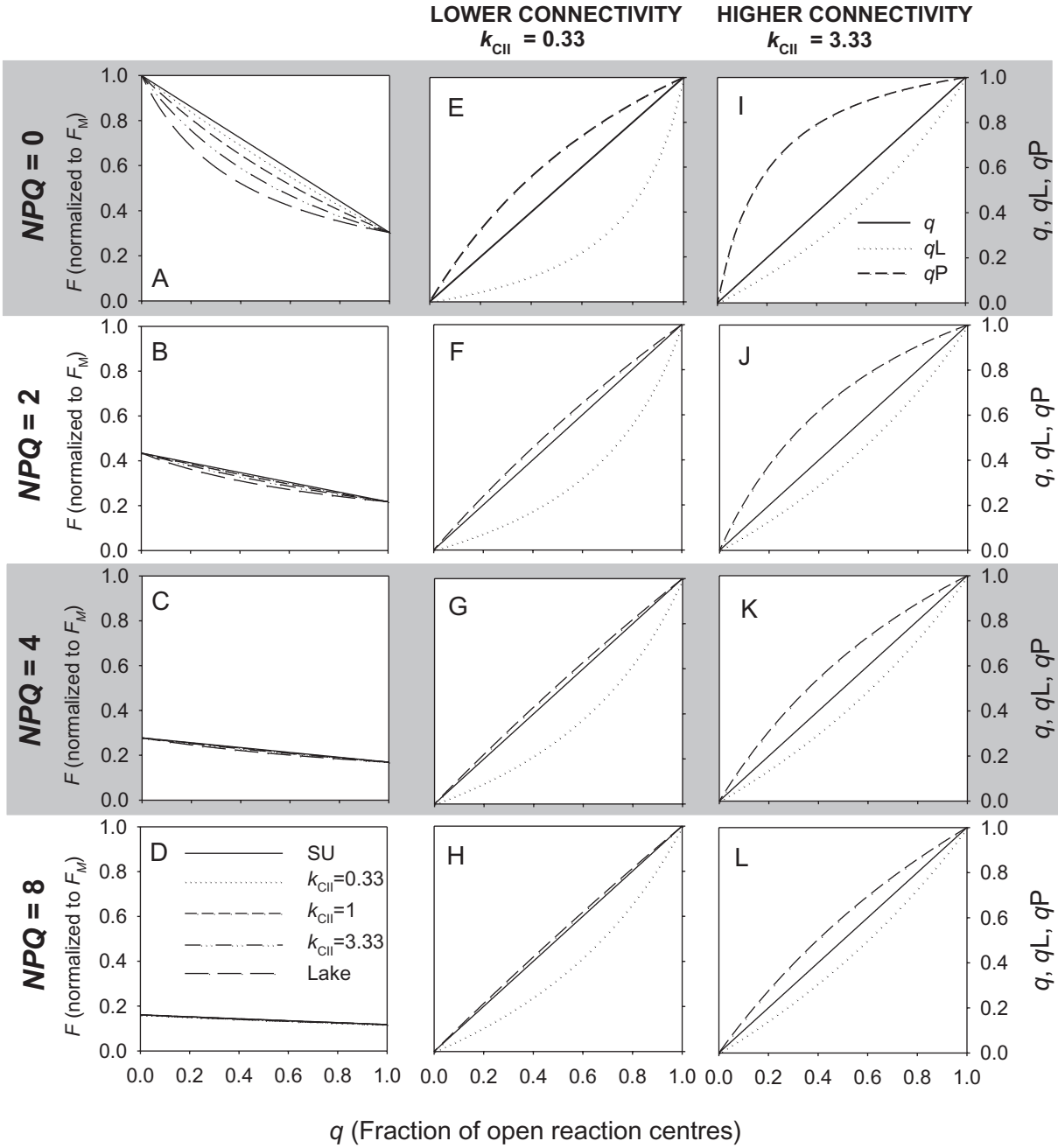

Fig. 5. Theoretical analysis of the interaction between photosystem II connectivity, the fraction of open reaction centres *q*, NPQ, and the parameters *q*L and *q*P. (A–D) The effect of increasing levels of NPQ on the relationship between *F* and *q* at different levels of connectivity, where k_{CII} is the rate constant of energy transfer between photosystems, ranging from zero, for the case of separate units (SU), to infinity, for a lake model. (E–L) Theoretical relationship between *q* and the fluorometric estimates of *q* based on a separate units assumption (*q*P) or on a lake model (*q*L) under different levels of NPQ and under two different connectivity scenarios. Derived using parameters and equations after Lavergne and Trissl (1995); see Appendix 1 for details.

commonly saturating light pulses (Schreiber *et al.*, 1986; see Section 4.1). The result is an increase in F_{II} to a maximal level (F_{IIM}). Where,

$$F_{IIM} = IAa_{II}\frac{k_F}{k_D + k_F + k_{NPQ}} \quad (8)$$

Since the sum of the quantum yields of all processes competing for excitation energy equals one, the quantum yield of photochemistry in PSII (ΦP) can be expressed in fluorescence terms as:

$$\Phi P = \frac{qLk_{PSII}}{k_D + k_F + k_{NPQ} + qLk_{PSII}} = 1 - \frac{k_D + k_F + k_{NPQ}}{k_D + k_F + k_{NPQ} + qLk_{PSII}} = 1 - \frac{\frac{k_F}{k_D + k_F + k_{NPQ} + qLk_{PSII}}}{\frac{k_F}{k_D + k_F + k_{NPQ}}} = 1 - \frac{F_{II}}{F_{IIm}} \quad (9)$$

which corresponds to the parameter derived by Genty *et al.*, (1989) at the level of PSII, and becomes ΦP_{max} (the widely used parameter F_V/F_M; see Section 4.1) when qL=1 and k_{NPQ}=0.

Because the rate constants k_D and k_F remain constant, variations in ΦP can be expressed as a function of photochemical and non-photochemical processes, with $k_D+k_F=1$. This simplification gives raise to the photochemical (PQ) and non-photochemical quenching (NPQ) parameters, where $\mathrm{PQ} = q\mathrm{L}\frac{k_{PSII}}{k_D + k_F}$ and $\mathrm{NPQ} = \frac{k_{NPQ}}{k_D + k_F}$ (Laisk *et al.*, 1997; Porcar-Castell, 2011), and the quantum yield of photochemistry can be expressed as:

$$\Phi P = \frac{\mathrm{PQ}}{1 + \mathrm{NPQ} + \mathrm{PQ}} \quad (10)$$

Note that the two forms of photochemical quenching parameter, PQ and qL, carry exactly the same information and can be used interchangeably depending on the application. For example, PQ facilitates the comparative analysis with NPQ because it has the same relative range of variation, whereas qL gives a more visual picture of the degree of reaction centre openness.

In contrast to PSII, the fluorescence yield of PSI is generally low and remains constant under illumination. Chlorophyll cations such as $P700^+$ and $P680^+$ are known to be very efficient in dissipating excitation energy as heat. However, in contrast to $P680^+$, the lifetime of $P700^+$ is longer and $P700^+$ operates as a very effective quencher of excitation energy in PSI (Dau, 1994; Lavergne and Trissl, 1995). The fluorescence spectral properties of PSII and PSI are also different (Fig. 6). At room temperature, ChlF from plant PSI presents a shoulder at 690 nm and a peak at 730 nm (Croce *et al.*, 1996), whereas fluorescence from PSII peaks at ~685 nm and presents vibrational satellite bands in wavelengths >700 nm (Govindjee, 1995) overlapping with PSI fluorescence (Franck *et al.*, 2002; Fig. 6). As a result of differences in yield and spectral properties between photosystems, PSI fluorescence has been found to contribute between 0 and 50% of total fluorescence depending on the method, measuring conditions, species, and especially the spectral region, with the contribution of PSI being insignificant in the red region and maximum in the near infrared (Fig. 6) (Genty *et al.*, 1990*b*; Dau, 1994; Pfündel, 1998; Agati *et al.*, 2000; Peterson *et al.*, 2001; Franck *et al.*, 2002; Palombi *et al.*, 2011; Pfündel *et al.*, 2013).

Analogously to PSII, we express the fluorescence flux emanating from a population of PSI units as:

$$F_I = IAa_I \frac{k_F}{k_D + k_F (+k_{NPQI}) + qk_{PSI} + k_{RCI}} \quad (11)$$

where a_I is the relative absorption cross-section area of PSI in the sample, q is the fraction of open PSI centres, k_{PSI} is the intrinsic rate constant of PSI photochemistry, and k_{RCI} is the rate constant of quenching by $P700^+$. Finally, k_{NPQI} is the rate constant of regulated thermal energy dissipation in PSI, the significance of which remains to be elucidated (see Section 5).

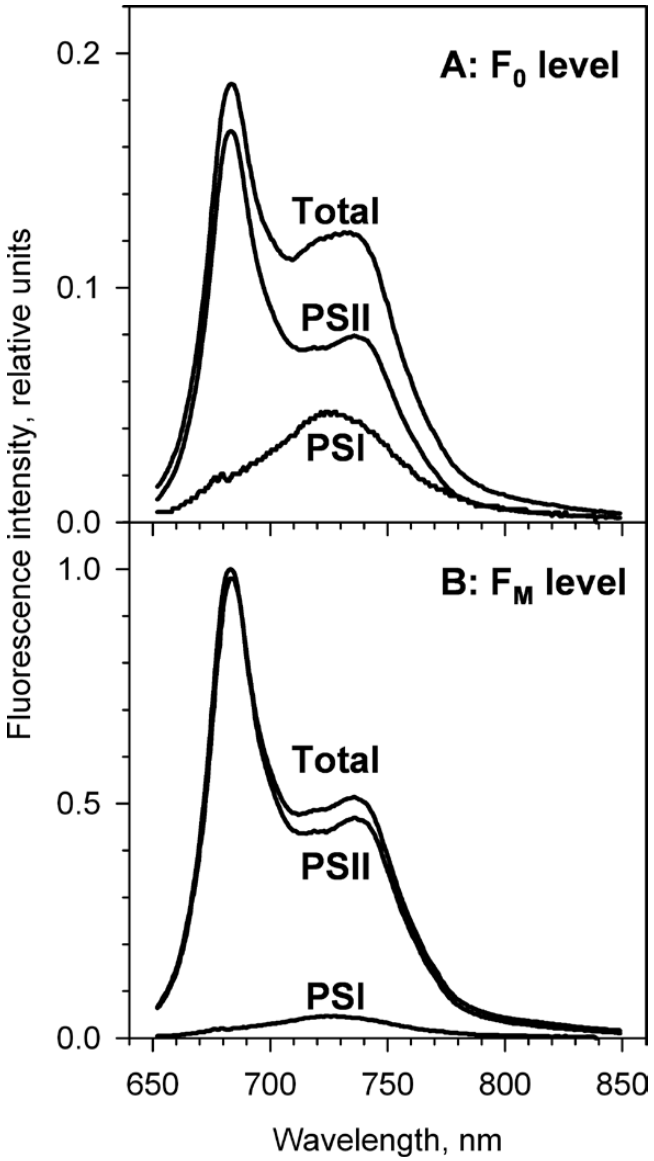

Fig. 6. The relative spectral contributions of PSI and PSII fluorescence to the total emission spectrum in barley leaves at the F_0 (A) and F_M (B) levels. Fluorescence is normalized to the peak in F_M. Redrawn after Franck F, Juneau P, Popovic R. 2002. Resolution of the photosystem I and photosystem II contributions to chlorophyll fluorescence of intact leaves at room temperature. *Biochimica et Biophysica Acta* 1556, 239–246. Copyright Elsevier 2002.

3.3 Chlorophyll fluorescence at the leaf level and beyond

A new set of factors and phenomena need to be considered when linking ChlF data and photosynthetic CO_2 assimilation at the leaf level and beyond (Fig. 4). The efficient absorption of blue and red light by chlorophyll within a leaf or by leaves within a plant canopy plays two important roles when scaling from the photosystem to the leaf level and beyond: (i) wavelength-dependent light penetration; and (ii) wavelength-dependent fluorescence reabsorption.

First, red light penetrates deeper into the leaf and is more scattered than blue light (Agati, 1998; Buschmann and Lichtenthaler, 1998; Vogelmann and Evans, 2002), whereas green light may have an optical path up to five times longer than that of red or blue light due to weaker absorption and higher scattering (Vogelmann, 1993; Rappaport *et al.*, 2007). Wavelength-dependent scattering and absorption within a leaf or a plant canopy generates important gradients in light quality and intensity which translate into similar gradients in thylakoid composition, stoichiometry, and physiological state. For example, the number of PSII reaction centres is known to increase with irradiance (Anderson *et al.*, 1988) or in response to far-red light (Chow *et al.*, 1990), whereas the antenna sizes of the photosystem (Melis, 1991; Anderson *et al.*, 1988; Ballottari *et al.*, 2007), as well as the absorption cross-section of PSII relative to PSI (Eichelmann *et al.*, 2005; Walters, 2005) both increase in response to shade. On the other hand, xanthophyll pigment pools and NPQ capacity are larger in sun-exposed compared with shaded foliage (Demmig-Adams, 1998; Niinemets *et al.*, 2003; Porcar-Castell *et al.*, 2008*a*). In addition, chloroplasts or leaves exposed to high light conditions tend to have lower photochemical efficiencies and larger NPQ compared with more shaded chloroplasts or leaves.

Secondly, because the spectra of ChlF emission overlaps with that of chlorophyll absorption, red fluorescence photons (F_R) can be reabsorbed by chlorophyll itself within the leaf or inside a plant canopy (Brody and Brody, 1962; Govindjee and Yang, 1966; Gitelson *et al.*, 1998). Reabsorption of F_R within the leaf can be as high as 90% (Gitelson *et al.*, 1998).

The overall result of the above two phenomena is that the biological footprint of a fluorescence measurement depends on the spectral properties of both the excitation light and the wavelengths across which fluorescence is retrieved (Fig. 7). The F_R signal (detected in the red region) is enriched in photosystems close to the leaf surface or leaves from the top of the canopy, whereas the F_{FR} signal (detected in the far-red) may have a stronger contribution from a deeper leaf or canopy layer, especially when the excitation light penetrates deep into the leaf or the canopy (Peterson *et al.*, 2001; Rappaport *et al.*, 2007; Pfündel, 2009). These differences are particularly relevant to the interpretation of SIF data where the signal can be obtained in different spectral regions that will consequently carry information from different layers of the leaf or the canopy (see Section 4.2).

Although Equations 6 and 7 provide the basis for linking ChlF and photochemistry, the effects of leaf and canopy structure also affect the ChlF signal and need consideration. A quantitative treatment of the impact of structure requires the use of leaf and canopy radiative transfer models. Here we use a simplified expression to introduce the main physical and physiological controls behind leaf-level ChlF (for similar formulations, see also Agati *et al.*, 1995; Dau and Sauer, 1996; Franck *et al.*, 2002; Pedrós *et al.*, 2008; Palombi *et al.*, 2011). The intensity and spectral properties of the chlorophyll fluorescence signal emanating from a leaf F can be represented (in µmol photons m^{-2} s^{-1} nm^{-1}) as:

$$\begin{aligned} &F\left[I(\lambda_{ex}), A(\lambda_{ex}), a_{II}(\lambda_{ex}), a_I(\lambda_{ex}), F_{PSII}(\lambda_{em}), \right. \\ &\left. F_{PSI}(\lambda_{em}), \mathrm{NPQ}, qL, p_r(\lambda_{em}, \mathrm{Chl}) \right] = \\ &I(\lambda_{ex}) A(\lambda_{ex}) \left[a_{II}(\lambda_{ex}) \Phi F_{II}(k_{NPQ}, qL) F_{PSII}(\lambda_{em}) + \right. \\ &\left. a_I(\lambda_{ex}) \Phi F_I F_{PSI}(\lambda_{em}) \right] \left[1 - p_r(\lambda_{em}, \mathrm{Chl}) \right] \end{aligned} \quad (12)$$

where $I(\lambda_{ex})$ and $A(\lambda_{ex})$ are the irradiance flux at the leaf surface and the leaf-level absorption as a function of the excitation wavelength; and $a_{II}(\lambda_{ex})$ and $a_I(\lambda_{ex})$ are the relative absorption cross-sections for each population of photosystems as a function of the excitation wavelength ($0 \le [a_{II}, a_I] \le 1$). For example, a_{II} and a_I were found to remain rather constant in spinach leaves for the range 400–680 nm, but a_I rapidly increases to 1 at > 675–680 nm (Kitajima and Butler, 1975*b*; Butler, 1978) where PSII no longer absorbs. $F_{PSII}(\lambda_{em})$ and $F_{PSI}(\lambda_{em})$ are the

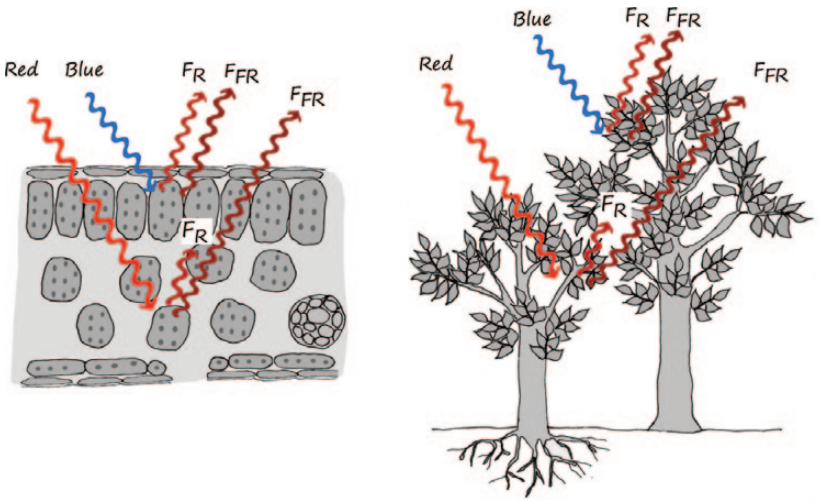

Fig. 7. Wavelength dependency of light penetration and fluorescence reabsorption within a leaf and a plant canopy. Red light penetrates deeper in the leaf or within a plant canopy compared with blue light due to higher scattering. In turn, red fluorescence (F_R) has a larger probability of being reabsorbed by chlorophyll within the leaf and canopy compared with far-red fluorescence (F_{FR}), due to the characteristics of the chlorophyll absorption spectra.

wavelength-dependent functions that account for the shape of the fluorescence emission spectra for PSII and PSI, respectively (Croce *et al.*, 1996; Franck *et al.*, 2002; Palombi *et al.*, 2011); and $p_r(\lambda_{em}, Chl)$ is a function that accounts for fluorescence reabsorption and depends on fluorescence wavelength, chlorophyll content, and leaf morphology. In the following, we use Equation 12 to discuss the differences between PAM and SIF fluorescence.

4. Measuring chlorophyll fluorescence

Two main methods are used to measure ChlF in the field: those based on PAM systems (active methods) and those based on the retrieval of SIF (passive methods). Although active methods based on laser technology have been also developed (e.g. Kolber *et al.*, 2005; Pieruschka *et al.*, 2010), their applicability at the canopy and landscape level remains to be assessed. More generally, active methods are applied at the leaf level whereas passive methods are being commonly applied at the canopy level and beyond. In the following, we describe the background of these measurements, their differences, and some of the underlying challenges. For further details, we suggest reviews by Maxwell and Johnson (2000), Schreiber (2004), or Baker (2008) for PAM fluorometry, or that of Meroni *et al.*, (2009) for SIF.

4.1 Pulse amplitude-modulated fluorescence

The main feature of PAM fluorometers is that a weak and pulsed measuring light (ML) is used to excite fluorescence (Duysens, 1979). Widths of measuring pulses are in the microsecond range and the pulse amplitude is constant. Pulse frequencies can range from 10 Hz up to 200 kHz depending on fluorometer and instrument setting. At low frequencies, dark intervals between measuring pulses are relatively long so that the average photon flux density of the ML is very small (<1 μmol m^{-2} s^{-1}) and does not cause any significant change in the degree of PSII openness (q) (see Section 3.2). PAM fluorometers subtract the fluorescence signal shortly before or after a measuring pulse from the fluorescence signal during this measuring pulse. This subtraction method is highly selective and eliminates virtually all non-PAM fluorescence from the measurement, for example the fluorescence excited by sunlight in field experiments. Because PAM fluorometers register only the fluorescence excited by this constant ML, variations in PAM fluorescence reflect variations in the efficiency by which the sample transforms modulated excitation light into fluorescence.

PAM fluorometers are characterized by the wavelength of the ML as well as the wavelength range at which modulated fluorescence is being registered. Recent advances in light-emitting diode (LED) technology allow PAM excitation in the entire visible range with a full width at half maximum (FWHM) between 20 nm and 40 nm. The spectral window for fluorescence detection is typically confined to wavelengths >700 nm using a long-pass colour filter, in order to minimize reabsorption effects. Using such filters, the PAM ChlF signal is typically integrated over tenths of nanometres, providing a broadband measure of ChlF. These characteristics differ from instrument to instrument.

Using 'Equation 12, the PAM fluorescence signal (F') in relative units (e.g. mV) emanating from a leaf under illumination can be expressed as:

$$F' = \beta I_{ML}(\lambda_{ML}) A(\lambda_{ML}) \left[a_{II}(\lambda_{ML}) \frac{k_f}{k_f + k_D + k_{NPQ} + qLk_{PSII}} F_{PSII}(\lambda_{retrieval}) + a_I(\lambda_{ML}) \Phi F_I F_{PSI}(\lambda_{retrieval}) \right] \left[1 - p_r(\lambda_{retrieval}, Chl) \right] \quad (13)$$

where β is a parameter that accounts for the properties and sensitivity of the detector system (e.g. mV m^2 s μmol photons^{-1}); $I_{ML}(\lambda_{ML})$ is the intensity of the PAM measuring light (μmol photons m^{-2} s^{-1}) with wavelength (λ_{ML}); $A(\lambda_{ML})$, $a_{II}(\lambda_{ML})$, and $a_I(\lambda_{ML})$ are the absorptance and relative absorption cross-section area of PSII and PSI, respectively, at the wavelength of the measuring light (λ_{ML}); and $F_{PSII}(\lambda_{retrieval})$ and $F_{PSI}(\lambda_{retrieval})$ account for the shape of the fluorescence emission spectra for PSII and PSI, respectively, averaged for the spectral range of the retrieval. ΦF_I is the fluorescence yield of PSI (see Equation 11) and $p_r(\lambda_{retrieval}, Chl)$ the average reabsorption probability for the wavelength range at which fluorescence is being retrieved and for the prevailing leaf morphology and chlorophyll content.

Equation 13 can be greatly simplified as a result of PAM design and by using a number of assumptions. (i) Because PAM fluorometers typically (but not always) register fluorescence >700 nm, we can assume they are not affected by reabsorption, i.e. $p_r(>700\,nm, Chl)=0$. (ii) Since the amplitude of the ML is constant, we can assume I_{ML}=constant. Therefore, at constant A and a_{II}, F' is proportional to $\Phi F'$. (iii) The contribution of PSI fluorescence to the total signal is usually assumed to be constant or negligible. (iv) The characteristic emission spectra for PSII and PSI are assumed to remain constant for the duration of the measurements [$F_{PSII}(\lambda_{retrieval})$ and $F_{PSI}(\lambda_{retrieval})$]. Indeed, because PAM ChlF is acquired over a broadband, the resulting signal is less likely to be affected by seasonal shifts in the fluorescence emission spectra compared with SIF. (v) $A(\lambda_{ML})$ and $a_{II}(\lambda_{ML})$ are often assumed to remain constant or their variation negligible. Given these simplifications, F' in Equation 13 corresponds to ΦF_{II} in Equation 7.

The operating quantum yield of photochemistry in PSII (ΦP) can be obtained by comparing the fluorescence level in the presence (F') (Equation 7) and in the absence (F'_M) of photochemistry (Equation 8). PAM fluorometers estimate maximal fluorescence (F'_M) by providing a pulse of saturating light (SP) for several hundreds of milliseconds (typically 0.6–1 s). The SP momentarily reduces all the electron acceptors of PSII so that primary photochemistry tends to zero and qL=0, and thus k_P=0 (Bradbury and Baker, 1981; Schreiber *et al.*, 1986). As a result F' increases to a maximal level F_M'. Accordingly, ΦP can be then estimated from PAM data following Equation 9, as:

$$\Phi P = 1 - \frac{\dfrac{k_F}{k_D + k_F + k_{NPQ} + qLk_{PSII}}}{\dfrac{k_F}{k_D + k_F + k_{NPQ}}} = 1 - \frac{F'}{F'_M} \quad (14)$$

Following from Equation 14 and provided that $I(\lambda)$, $A(\lambda)$, and $a_{II}(\lambda)$ are known for the range 400–700 nm (PAR), the rate of LET through PSII can be estimated as (Genty *et al.*, 1989; Schreiber, 2004; Baker, 2008):

$$\mathrm{ETR} = I(\mathrm{PAR})\, A(\mathrm{PAR})\, a_{II}(\mathrm{PAR})\ \Phi P \quad (15)$$

Commercial fluorometers usually provide an estimate of the electron transport rate (ETR) by assuming that PAR leaf absorptance equals 0.84 (Baker, 2008) and that absorbed photons are equally distributed between the two photosystems (i.e. a_{II}=0.5). This approximation is reasonable for comparison of ETR values between optically similar samples such as leaves of cultivars of a single plant species. When the data expand over several species or extend to a long time period, then the significance of species-specific, within-canopy gradients or seasonal variation in A and a_{II} need to be taken into account when calculating ETR. The same applies to other fluorescence parameters (Baker and Oxborough, 2004; Logan *et al.*, 2007).

Other important fluorescence parameters can be estimated by dark-acclimating the leaf for a period of time (15 min to 2 h). The purpose of dark acclimation is to re-oxidize the Q_A electron acceptors in every PSII (which takes only several seconds) and to relax all the reversible NPQ, which may take a few minutes or hours, depending on temperature (Bilger and Björkman, 1991; Eskling, 1997; Demmig-Adams and Adams, 2006). By definition, dark acclimation of sufficient length decreases NPQ to zero, k_{NPQ}=0 in Equation 8. Under these conditions, minimal (F_0) and maximal (F_M) fluorescence levels of the dark-acclimated leaf are obtained.

Substituting F' by F_0 (i.e. qL approaches unity), and F_M' by F_M (i.e. NPQ approaches zero), we can use Equation 14 to estimate the maximum quantum yield of photochemistry (ΦP_{max}), as (Kitajima and Butler, 1975*a*):

$$\Phi P_{max} = 1 - \frac{F_0}{F_M} = \frac{F_M - F_0}{F_M} = \frac{F_V}{F_M} \quad (16)$$

The F_V/F_M parameter or ΦP_{max} has been found to remain rather constant in non-stressed C_3 plants, with values of ~0.83 (Björkman and Demmig, 1987). Consequently, a decrease in F_V/F_M below the value found in healthy plants of the same species has been used as an indicator of decreased photochemical performance caused, for example, by photoinhibition of reaction centres or sustained forms of NPQ (Ottander, 1991; Adams and Demmig-Adams, 2004; Ensminger *et al.*, 2004; Porcar-Castell *et al.* 2008*a*, *b*).

Provided that factors such as light absorptance (A) and PSII relative absorption cross-section (a_{II}) remain constant, differences between F_M' and F_M can be used to estimate the regulated non-photochemical quenching or NPQ, via the parameter NPQ (Bilger and Björkman, 1991):

$$NPQ = \frac{k_{NPQ}}{k_F + k_D} = \frac{F_M - F'_M}{F'_M} \quad (17)$$

Similarly, F', F_M', and F_M can be combined to estimate the photochemical quenching or PQ, via the parameter PQ (Porcar-Castell, 2011):

$$PQ = qL\frac{k_{PSII}}{k_F + k_D} = \frac{F_M}{F'} - \frac{F_M}{F'_M} \quad (18)$$

These are just some of the many parameters that can be obtained using PAM fluorescence. Further photochemical and non-photochemical quenching parameters and process quantum yields can be found elsewhere (e.g. Roháček, 2002; Krause and Jahns, 2004; Schreiber, 2004; Baker, 2008; Porcar-Castell, 2011).

When the underlying assumptions are carefully considered (Maxwell and Johnson, 2000; Logan *et al.*, 2007; Baker, 2008), PAM fluorometry becomes a very versatile tool that provides highly informative data to track the acclimation of the light reactions of photosynthesis. PAM fluorometry also provides the possibility of studying in detail and modelling the link between ChlF and photosynthesis in the new spatiotemporal domain (seasonal, within-canopy, multiple species). We expect that the rapid spread of gas exchange systems combined with PAM fluorometers, the recent availability of long-term PAM monitoring systems (Porcar-Castell *et al.*, 2008*c*; Porcar-Castell, 2011), and the development of other active techniques such as the laser-induced fluorescence transient (LIFT) (Kolber *et al.*, 2005; Pieruschka *et al.*, 2010) will favour these developments.

4.2 Solar-induced fluorescence and passive remote sensing

SIF is chlorophyll fluorescence that originates from excitations caused by the absorption of sunlight. SIF can be measured using passive remote sensing at a range of scales; from leaves in the laboratory (Gamon 1990) to satellite-based retrievals across the landscape (Guanter *et al.*, 2007; Frankenberg *et al.*, 2011; Joiner *et al.*, 2011). As discussed in the Section 4.1, PAM fluorometers measure fluorescence induced by a (modulating) ML source which makes the observations independent from any other irradiance source (such as the sun). In contrast, careful characterization of the incident irradiance field is required if SIF-based ChlF observations are to be meaningfully compared with PAM fluorescence measurements.

The principal passive remote sensing technique used to estimate SIF is the Fraunhofer line depth/discriminator (FLD) method (Plascyk, 1975). Fraunhofer lines are dark, narrow regions of the solar spectrum that are caused by gaseous absorption in the Sun's photosphere. There are also several dark regions in the spectrum caused by gaseous absorption in the Earth's atmosphere, so-called telluric lines. Several Fraunhofer and telluric lines are found at wavelengths coincident with fluorescence emission and are literally filled in by fluorescence (examples are shown as grey vertical lines

on Fig. 8A). In reality, several spectrally adjacent lines may contribute to a specific Fraunhofer 'feature'. It is across these features that the FLD algorithm is applied [in a slight abuse of terminology, we use 'line(s)' and 'feature' interchangeably in this section].

Changes in the fractional depths of Fraunhofer lines are used as the foundation of the FLD retrieval. In essence, the relatively weak fluorescence signal is amplified in these features of the spectrum. The FLD method can be applied to many different lines including the Fraunhofer hydrogen-α band (656 nm), potassium D1 (769nm), the telluric oxygen-B (690 nm), and oxygen-A (760 nm) bands. To compute SIF using the FLD method it is not necessary to measure whole radiance or irradiance spectra; rather, four measurements are needed in total. One measurement of solar irradiance and target radiance is taken 'inside' the line, and one measurement of solar irradiance and spectral radiance is taken directly next to the line. The following expression is used to retrieve fluorescence across the line ($SIF_{\lambda retrieval}$):

$$SIF_{\lambda retrieval} = \frac{L_{inside}E_{outside} - L_{outside}E_{inside}}{L_{inside} - E_{outside}} \quad (19)$$

L and E refer to radiance and irradiance measurements taken at a wavelength within (inside) and outsidea particular line feature. The key assumption is that the bands are sufficiently close so that both inherent reflectance and fluorescence are constant across the lines. In practice, these assumptions are often violated, which has motivated the development of several improved FLD-based retrievals [see the description of the spectral fitting method below, and Meroni (2009) for an in-depth review of improved methods].

The physiological interpretation of the resulting SIF signal depends on the spectral line chosen for the retrieval, $SIF_{\lambda retrieval}$. Consistent with PAM fluorescence (Equation 13), the SIF signal can be expressed using Equation 11 for a specific retrieval wavelength, as:

$$SIF_{\lambda retrieval} = \int_{\lambda_{sun}=400}^{\lambda_{sun}=700} I(\lambda_{sun})A(\lambda_{sun})\left[a_{II}(\lambda_{sun})\Phi F_{II}F_{PSII}(\lambda_{retrieval}) + a_{I}(\lambda_{sun})\ \Phi F_{I}\ F_{PSI}(\lambda_{retrieval})\right]\left[1 - p_r(\lambda_{retrieval}, Chl)\right]\ d\lambda_{sun} \quad (20)$$

From Equation 20 it is evident that the interpretation of the resulting SIF signal depends on the spectral window chosen to retrieve SIF. The SIF signal measured at the O_2B line, SIF_{690}, is very close to the chlorophyll absorption peak and is therefore very sensitive to reabsorption of fluorescence by chlorophyll. This is not the case for SIF_{760} which is measured in the O_2A line. Therefore, the SIF signal carries different physical–physiological information depending on the region used in the retrieval (Fig. 7). In addition, the contribution from PSI fluorescence will also vary depending on the retrieval line wavelength. This is due to differences in wavelength dependencies of $F_{PSII}(\lambda_{retrieval})$ and $F_{PSI}(\lambda_{retrieval})$ in Equation 20 which cause a higher relative contribution of PSI fluorescence at longer wavelengths since $F_{PSII}(690) >> F_{PSII}(760)$ (Fig. 6). A further challenge faced when retrieving SIF from space is accurately correcting for atmospheric scattering and absorption effects. These may act to modify the observed SIF signal. In particular, when using telluric lines to retrieve SIF, the same chemical species that absorbs solar irradiance in the Earth's atmosphere (causing the feature) also absorbs the emitted SIF signal. This means that precise atmospheric correction is essential if accurate canopy-leaving estimates of SIF are to be retrieved from at-sensor observations.

A promising development of the FLD method is the spectral fitting method (SFM) (Meroni *et al.*, 2009). The SFM solves the inverse problem of estimating fluorescence across a Fraunhofer feature by using a least-squares approach. In the SFM, FLD observations are fitted with synthetic spectra modelled using simple polynomial functions. The SFM was designed to reduce noise and to be more robust to contamination by atmospheric effects than the FLD method and was demonstrated to increase the accuracy of SIF retrievals in comparison with the basic FLD algorithm (Meroni *et al.*, 2009).

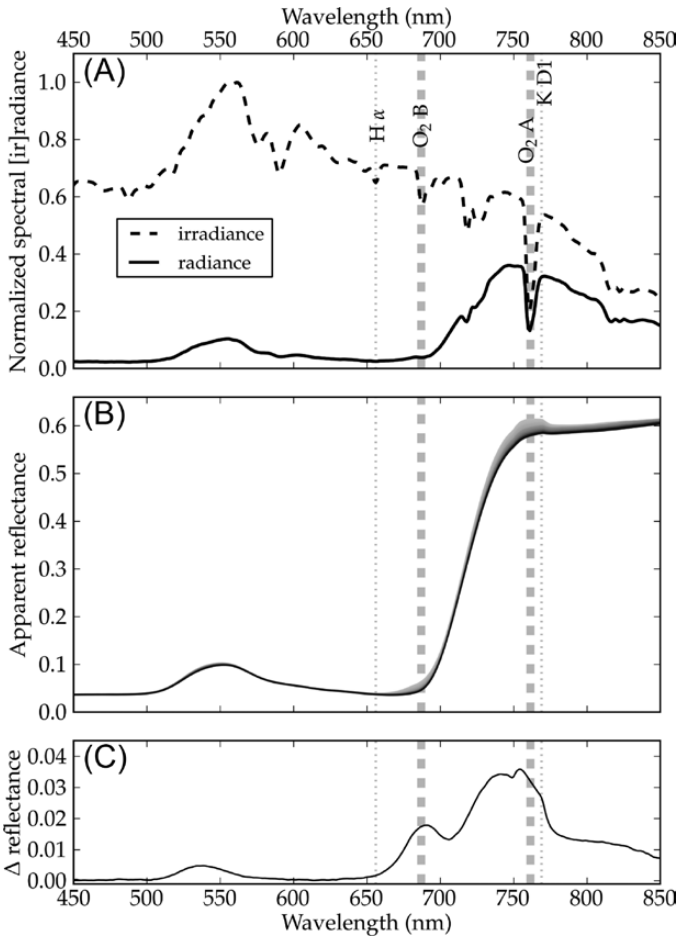

Fig. 8. Leaf spectral reflectance including the solar-induced fluorescence contribution. Incoming solar irradiance and spectral radiance of a maple (*Acer* sp.) leaf, measured using an ASD-HH Field Spec spectroradiometer (ASD Inc., USA). Hydrogen and oxygen absorption bands are highlighted in grey (A). Temporal dynamics in spectral reflectance measurements upon exposure of a dark-adapted maple leaf to full sunlight over 3 min. The rapid fluorescence dynamics are shown in grey, and the black line denotes the steady-state spectrum after a few minutes of illumination (B). (C) The difference between the first and last reflectance spectra from the middle panel. The large peak in the difference spectrum in the near-infrared wavelengths denotes the spectral properties of the dynamic (variable) fluorescence (J. Atherton *et al.*, unpublished data).

In addition to FLD-based methods, reflectance spectroscopy can be used to gain insight into the relationship between ChlF and photosynthesis. This is because the fluorescence emission spectrum is superimposed on the leaf (or canopy) reflectance spectrum. The reflectance spectrum is measured, typically in the laboratory or the field, as the ratio of reflected radiance to incident irradiance using hyperspectral spectroradiometers (Fig. 8B). A number of reflectance band ratios (algebraic combinations of ≥2 narrow spectral reflectance 'bands') have been developed to quantify the effect of fluorescence emission on the reflectance spectrum (Meroni *et al.*, 2009). These methods are particularly popular at the leaf scale where they are often compared and contrasted to reflectance indices that measure related physiological processes such as the photochemical reflectance index (PRI) (Gamon *et al.*, 1992) or chlorophyll-based indices (Richardson and Berlyn, 2002). Reflectance difference spectra are useful as measures of the dynamic fluorescence contribution to reflectance. Difference spectra can be calculated from sets of reflectance spectra both as a function of time (Gamon *et al.*, 1990) and using a filter-based approach (Zarco-Tejada *et al.*, 2000; Campbell *et al.*, 2008; Meroni *et al.*, 2009). Filter-based approaches are used to extricate the chlorophyll fluorescence contribution from the measured apparent reflectance spectrum.

5. Remaining challenges: from diurnal to seasonal, from the leaf to the landscape, from active to passive fluorescence.

Time-resolved fluorescence spectra and lifetime analysis have proved essential for elucidating structural and functional features of photosynthesis (Roelofs *et al.*, 1992; Dau, 1994; Govindjee, 1995; Croce *et al.*, 1996; Lázar, 1999; Jennings *et al.*, 2003; Vassiliev and Bruce, 2008). Likewise, PAM fluorescence measurements have been valuable in studying the ecophysiology of photosynthesis at the leaf level and *in situ* (Bradbury and Baker, 1991; Ottander *et al.*, 1991; Adams and Demmig-Adams, 1994; Verhoeven *et al.*, 1996; Ogaya and Peñuelas, 2003; Ensminger *et al.*, 2004; Porcar-Castell *et al.*, 2008*a*, *b*, *c*; Porcar-Castell, 2011).

The ChlF signal is now being applied to the study of photosynthesis from remote sensing platforms. Before we can mechanistically link SIF and GPP, we need to expand the knowledge we have gained from short-term measurements using mainly PAM techniques at leaf level, to the seasonal and canopy level using SIF instead. This involves a number of challenges that are introduced in this section and can be summarized as follows. (i) Temporal up-scaling. Factors that control the seasonal variation of ChlF properties remain unclear. (ii) Spatial up-scaling. In addition to characterizing and modelling the radiative transfer of the signal, up-scaling from the leaf to the landscape also requires understanding of the vertical and species-specific variation in physiological traits, an area with very limited information. (iii) Mechanistic up-scaling from SIF to gross photosynthesis. In contrast to PAM fluorescence, the quantum yield of photochemistry cannot be directly resolved from SIF. This problem can only be bypassed by developing robust models to link SIF to GPP, an area where a quantum leap forward is urgently needed.

5.1 Temporal up-scaling: from the diurnal to the seasonal scale

Over the short term (seconds to days) it is reasonable to assume that most of the factors that control the ChlF signal at the leaf level (Equation 12) remain constant, so that variations in fluorescence can be largely attributed to photochemical or non-photochemical processes in PSII (i.e. qL and NPQ) (Maxwell and Johnson, 2000; Logan *et al.*, 2007; Baker, 2008), as well as to changes in illumination $I(\lambda_{ex})$ in the case of SIF. However, it remains largely unknown whether these simplifying assumptions hold at the seasonal scale (days to months).

Changes in chlorophyll contents, leaf absorptance, and fluorescence reabsorption

Leaf chlorophyll concentrations vary at the seasonal time scale (García-Plazaola and Becerril, 2001; Lu *et al.*, 2001). This is particularly evident during leaf development and senescence, but adjustments in pigment concentrations occur also in evergreen foliage during the course of the seasons. For example, boreal Scots pine trees decrease their needle chlorophyll concentration by up to ~40% in winter compared with summer (Ensminger *et al.*, 2004; Porcar-Castell *et al.*, 2012). An increase in leaf-level chlorophyll content may have mixed effects on ChlF.

Chlorophyll concentration modulates light absorptance $A(\lambda)$ and, by extension, ChlF (Equation 12). The relationship between chlorophyll content and light absorptance is positive and non-linear, saturating at high chlorophyll contents (Björkman and Demmig, 1987; Adams *et al.*, 1990; Gitelson *et al.*, 1998). In agreement with this, the relationship between leaf-level chlorophyll concentration and the fluorescence signal also saturates at high chlorophyll contents (Adams *et al.*, 1990).

Similarly, chlorophyll concentration also modulates fluorescence reabsorption (Equation 12) and, by extension, ChlF. An increase in absorption $A(\lambda)$ will cause an increase in fluorescence at all wavelengths, whereas an increase in reabsorption will decrease red but not far-red ChlF (Lichtenthaler and Rinderle, 1988; Gitelson *et al.*, 1998). This phenomenon is built in the ratio of red to far-red fluorescence (F_R/F_{FR}) to estimate chlorophyll concentrations. Interestingly, the processes controlling F_R/F_{FR} depend on scale. At the diurnal scale, F_R/F_{FR} varies in response to the action of NPQ (Agati *et al.*, 1995), whereas at the seasonal scale or when comparing leaves with different chlorophyll contents, F_R/F_{FR} reflects changes in chlorophyll concentration (Lichtenthaler and Rinderle, 1988; Gitelson *et al.*, 1998). This scale-dependent relationship also affects the correlation between F_R/F_{FR} and LUE. The ratio F_R/F_{FR} is directly proportional to LUE over the diurnal scale (Agati *et al.*, 1995), but becomes inversely proportional to LUE at the seasonal scale (Freedman

et al., 2002), emphasizing the importance of scale when interpreting data.

Leaf chlorophyll concentration is therefore expected to have a mixed effect on the ChlF signal, with absorption effects dominating in leaves with low chlorophyll concentrations (i.e. more chlorophyll more fluorescence), and reabsorption effects dominating in leaves with high chlorophyll contents (i.e. more chlorophyll less fluorescence) (unless PAM fluorometer design discriminates all red fluorescence). This is consistent with results obtained in *Hedera canariensis* and *Platanus occidentalis* where the shift from absorption- to reabsorption-dominated effects took place at chlorophyll concentrations around 250 mg Chl m^{-2} (Björkman and Demmig, 1987; Adams *et al.*, 1990). Further characterization of the interplay between chlorophyll contents, leaf absorption, and wavelenght-dependent fluorescence properties across leaves with different morphologies is warranted to model these effects

Changes in relative absorption cross-sections of PSII (a_{II}) and PSI (a_I)

PSII and PSI have different fluorescent properties. The quantum yield of PSI (ΦF_I) is typically much smaller than ΦF_{II}, and PSI fluorescence peaks at longer wavelengths than PSII fluorescence (Fig. 6). Consequently, changes in the relative absorption cross-sections of PSII (a_{II}) and PSI (a_I) affect the fluorescence yield and spectra of the leaf. Over the short term, state transitions are known to reduce a_{II} and increase a_I, and, since $\Phi F_I < \Phi F_{II}$, the intensity of the fluorescence signal decreases. This quenching has been described in PAM fluorescence terms as qT (Krause and Weis, 1991), although qT does not contribute to NPQ as such (non-radiative quenching of excitation energy in PSII) but simply quenches F' by decreasing a_{II}, which results in a decrease in F_M' (Equation 8) and a subsequent increase in the parameter NPQ (Equation 17). In addition, state transitions also produce a change in the spectral properties of the F signal, with F_R being decreased to a larger proportion than F_{FR} due to a larger contribution of PSII fluorescence in the red relative to far-red. This phenomenon is particularly visible at liquid nitrogen temperature (77 °K) when the PSII and PSI fluorescence peaks can be separated, with F_R (originating mainly in PSII) and F_{FR} (originating mainly in PSI) (Butler, 1978; Govindjee, 1995). Changes in the 77 °K fluorescence ratio F_R/F_{FR} have been used to study state transitions (e.g. Tan *et al.*, 1998).

The question is, how stable/dynamic are the relative absorption cross-sections at the seasonal scale? If a_{II} and a_I would change over the season, we could expect a similar effect to that of state transitions, and possibly modifications in the relationship between ChlF, NPQ, and photochemistry. Direct measurement of the relative absorption cross-sections of PSII and PSI remains a challenge (Laisk *et al.*, 2002; Eichelmann *et al.*, 2005). Studies that directly measure a_{II} and a_I in conjunction with fluorescence spectral properties at the seasonal scale will help elucidate the dynamics and impact of a_{II} and a_I on ChlF.

Down-regulation of photosynthesis

Leaf-level fluorescence spectra might also change in response to the structural re-organization of the thylakoid observed, for example, in response to low temperature. The aggregation of LHCs in PSII has been suggested to be part of the mechanism of sustained stress-induced down-regulation of PSII (Ottander *et al.*, 1995; Ensminger *et al.*, 2004; Verhoeven, 2014). Winter down-regulation of the photosystem is known to be accompanied by up-regulation in SpsB proteins and xanthophyll cycle pigments (Ensminger *et al.*, 2004; Zarter *et al.*, 2006). These sustained quenching phenomena enhance NPQ and decrease the quantum yield of fluorescence and photochemistry, but also induce changes in fluorescence spectra. Gilmore and Ball (2000) identified what they called the cold-hard band (CHB) in overwintering snow gum leaves, where they showed that the leaf fluorescence spectrum was blue-shifted (i.e. moved towards shorter wavelengths) in response to cold acclimation. Interestingly, the CHB was shown to be fully reversible under constant chlorophyll content during recovery, suggesting that NPQ and perhaps also fluorescence spectra of the photosystems, $F_{PSII}(\lambda_{em})$ and $F_{PS}I(\lambda_{em})$, modulate the fluorescence spectral properties during down-regulation episodes. Measuring the fluorescence spectral properties of leaves and isolated PSII units under different levels and forms of NPQ (i.e. reversible and sustained) could serve to study how fluorescence spectra change in response to down-regulation of photosynthesis and its impact on both PAM and SIF fluorescence.

Effect of temperature

Long-term field observations (such as those in remote sensing) are often conducted under a wide range of temperatures that can easily exceed 60 °C. The yield and shape of the fluorescence spectrum are known to change in a thermodynamic process that takes place independently of plant physiological status (Croce *et al.*, 1996; Gobets and van Grondelle, 2001). When temperature is decreased from ambient to liquid nitrogen temperature (77 °K) the fluorescence yield of PSI ΦF_I increases because excitations are trapped in the so-called red chlorophylls (Croce *et al.*, 1996; Gobets and van Grondelle, 2001; Jennings *et al.*, 2003).

Red chlorophylls absorb at longer wavelengths than the rest of the antenna, but, at physiological temperatures, uphill energy transfer from the red chlorophylls to the bulk antenna is possible through thermal activation using vibrational energy from the phonon bath (i.e. energy contained in the vibrations of the pigment–protein matrix) (Jennings *et al.*, 2003; van Grondelle and Novoderezhkin, 2006). At low temperature (e.g. 77 °K), the phonon bath does not provide sufficient energy for the uphill energy transfer (Jennings *et al.*, 2003), and excitations get trapped in these chlorophylls, giving rise to an increase in fluorescence yield as well as a slight red shift in peak position (Croce *et al.*, 1996). Low temperature also limits energy transfer between PSII proteins, and two spectral peaks or shoulders (685 nm and 695 nm) appear at 77 °K instead of one single peak observed at room temperature (Govindjee, 1995; Keränen *et al.*, 1999; Maxwell and Johnson, 2000).

Because these thermodynamic effects take place gradually between ambient and liquid nitrogen temperature (Brody and Brody, 1962; Gylle *et al.*, 2012), they may need consideration when analysing ChlF data sets collected under a wide range of temperatures. For example, the ChlF of a *Chlorella* sp. suspension increased by 30% when lowering temperature from 25 ºC to –30 ºC at 720 nm (Brody and Brody, 1962). In addition, the differential dependence of both F_0 and F_M on temperature at a physiologically relevant range has also been observed in leaves (Weis and Berry, 1988; Kuropatwa *et al.*, 1992; Pospíšil et al., 1998). Similar increases in ChlF in both the red and near infrared with decreasing temperature have been observed in intact leaves (e.g. Agati, 1998; Agati *et al.*, 2000). Physiological and thermodynamic effects cannot always be decoupled empirically, although physiological factors determine the differential effect on F_0 and F_M (Pospíšil et al., 1998) or the dependence of the temperature effect on the needle age found in spruce (Ilík *et al.*, 1997). The impact and seasonal dynamics of the thermodynamic phenomena deserve to be quantified and characterized with dedicated experiments using various species and leaves presenting different physiological states, so that the effect can be modelled and corrected if needed.

Seasonal changes in connectivity between PSII units

Connectivity is the phenomenon by which excitation energy moves between neighbouring photosystems. This affects the relationship between fluorescence and the fraction of open/functional reaction centres (q) (Fig. 5) (Joliot and Joliot, 1964; Havaux *et al.*, 1991; Lavergne and Trissl, 1995; Kramer *et al.*, 2004*b*). In the absence of connectivity (separate units model), fluorescence yield is linearly related to q (Fig. 5A). In contrast, a system with connected PSII units will result in lower fluorescence yield for the same levels of reaction centre closure (q), because excitation energy in closed reaction centres can be quenched by neighbouring open reaction centres. Therefore, changes in connectivity *per se* can generate a change in ΦF at constant q and NPQ, complicating the interpretation of ChlF data. Connectivity between PSII units has been shown to change in response to protein phosphorylation (Kyle *et al.*, 1982), salt stress (Mehta *et al.*, 2010), and thylakoid grana stacking (Chow *et al.*, 2005). Because the impact of connectivity on ChlF decreases with NPQ (Fig. 5A–D), and because SIF is by default measured under illumination in the presence of NPQ, it is likely that connectivity and its potential dynamics do not exert a significant control on SIF. However, because seasonal changes in connectivity are likely to occur, the lake model assumption requires validation at the seasonal scale. The potential impact of seasonal changes in connectivity needs to be considered when attributing changes in photochemical quenching parameters such as qP or qL to processes such as photoinhibition of reaction centres, or when a connectivity assumption is used to derive fluorescence parameters as in the LIFT approach (Kolber *et al.*, 2005).

The contribution of PSI fluorescence to total fluorescence

The dynamics of the ChlF signal are most often associated with PSII and used to derive information on the acclimation of PSII. PSI has been typically ignored or corrected for using a constant offset value. Using different techniques and species, the contribution of PSI fluorescence has been found to range from close to zero in the red portion of the fluorescence spectra and up to 50% (Genty *et al.*, 1990*b*; Dau, 1994; Pfündel, 1998; Agati *et al.*, 2000; Peterson *et al.*, 2001; Franck *et al.*, 2002; Palombi *et al.*, 2011; Pfündel *et al.*, 2013). Franck *et al.* (2002) presented a method to resolve the spectral fluorescence contribution at the F_0 and F_M states (Fig. 6) that illustrates the wavelength dependency of the PSI fluorescence contribution. The contribution of PSI to total fluorescence decreases with decreasing photochemical quenching in PSII, becoming relatively insignificant at the F_M level (q=0). Under natural illumination F' and SIF levels are typically much closer to F_0 than to F_M, and the contribution that should be taken as reference of PSI fluorescence 'offset' is that obtained at the F_0 level and not the F_M. Clearly, PSI contribution to total fluorescence is important and cannot be ignored. However, can we expect this ChlF 'offset' to remain constant over time?

There are three different mechanisms by which PSI fluorescence contribution can vary. (i) Changes in chlorophyll content affect reabsorption of F_R (Lichtenthaler and Rinderle, 1988; Gitelson *et al.*, 1998). Consequently, because the red region is enriched in PSII fluorescence (Fig. 6), increasing chlorophyll contents will tend to increase the overall PSI fluorescence contribution. (ii) PSI contribution might dramatically increase in response to sustained NPQ and down-regulation of PSII. Although F_0 represents a theoretical minimal fluorescence, fluorescence is known to decrease below summer/non-stressed F_0 levels when the photosystems are deeply down-regulated (Porcar-Castell *et al.*, 2008*a*; Soukupová *et al.*, 2008; Porcar-Castell, 2011). Under these conditions, and unless sustained forms of NPQ operate in a similar fashion in both photosystems, the contribution of PSI fluorescence to the total signal could dramatically increase relative to the contribution estimated at the summer F_0. Finally, (iii) seasonal changes in the relative absorption cross-sections of PSII and PSI would equally affect PSI contribution. The seasonal dynamics in the PSI contribution to the total ChlF signal await further study so that we can relate the seasonal changes in the ChlF signal to processes taking place only in PSII, or in both photosystems.

In particular, the significance of sustained forms of NPQ in PSI and its putative impact on ΦF_I remain controversial. On one hand, there is no evidence of a significant effect of NPQ on PSI fluorescence over the short term (Genty *et al.*, 1990*b*; Krause and Jahns, 2004; Pfündel *et al.*, 2013), although it is known that 30–50% of the xanthophyll cycle pigments are associated with PSI, and de-epoxidation reactions also take place in PSI (Thayer and Björkman, 1992; Lee and Thornber, 1995; Färber, 1997). In contrast, NPQ has been found to have no effect on the redox state of the electron transport chain (Tikkanen *et al.*, 2011), which suggests that NPQ might operate in an equal fashion in both photosystems, unless CET is highly dynamic. The hypothesis of a constant ΦF_I awaits validation at the seasonal scale.

5.2 Spatial up-scaling

With the development of ChlF measurement techniques that can monitor targets of different size (leaf, canopy, and landscape), the question of scaling of process knowledge becomes increasingly important (Fig. 4). One of the main challenges in up-scaling is how to represent the spatial variability in physical and physiological factors within a leaf or a plant canopy (Malenovský *et al.*, 2009). When measuring SIF emitted by a leaf, the resulting signal can be expected to emanate predominantly from the top layers which are exposed to higher irradiance levels, as discussed in Section 3.3. Similarly, when measuring SIF of a plant canopy, the SIF signal will mainly consist of fluorescence originating from the top of the canopy, which is exposed to higher irradiance. For canopy-level observations, an additional problem is that the signal depends on canopy structure, sun elevation, and view angle, with different fractions of sunlit and shaded leaves visible from the perspective of the observer when looking at the same canopy from different angles. SIF thus depends on the position of the observer, whereas the emission at the photosystem level does not (van der Tol *et al.*, 2009).

Similarly, as discussed in Section 3.3, the fact that the resulting fluorescence signal needs to travel through a variable depth of leaf or canopy before it reaches the sensor will change the spectral properties of the signal due to variable and selective reabsorption of red fluorescence (Gitelson *et al.*, 1998; Franck *et al.*, 2002). The signal will be enriched in top canopy leaves for SIF (red), for example SIF_{690}, with a larger contribution from leaves deeper in the canopy for SIF (far-red), for example SIF_{760}. Daumard *et al.* (2012) analysed measurements of top-of-canopy SIF in a crop in the red and far-red during an entire season, and concluded that the far-red contains clear information about the development and photosynthetic capacity of the crop, whereas the F_R/F_{FR} ratio was sensitive to chlorophyll concentrations and the structure of the vegetation.

Radiative transfer models have been developed to simulate the effects of leaf and canopy structure and geometry on the wavelength-dependent radiative fluxes, ranging from simple turbid medium approaches (Allen, 1964) to ray tracing in realistic vegetation models (Gastellu-Etchegorry *et al.*, 2004). Of intermediate complexity (and realism) are models that treat the canopy as a stochastically distributed arrangement of leaves (Verhoef, 1984). Some of these models also include the radiative transfer of ChlF emission in leaves (Pedrós *et al.*, 2010) and canopies (Rosema *et al.*, 1998; Miller *et al.*, 2005; van der Tol *et al.*, 2009; Zarco-Tejada *et al.*, 2013). These models are designed to reproduce the fate of the emitted ChlF spectra through the leaf and canopy. It is not yet known how accurately these models represent the structural effects of vegetation on observations of SIF, or how sensitive they are to the underlying assumptions of leaf and canopy structure.

In addition to understanding radiative transfer as a physical process (physical modelling), we also need to solve the question of how physiological traits and photosynthesis dynamics (Equation 12) control the resulting fluorescence signal (physiological modelling). Understanding this aspect requires coupling radiative transfer with physiology. Models that couple radiative transfer and photosynthesis have been used for decades (Sellers, 1985; Goudriaan, 1988), but SIF has been only recently included (Miller *et al.*, 2005; van der Tol *et al.*, 2009). Even though these models have already been implemented for certain real-world scenarios, it remains unknown how well they represent the interactions between illumination and physiology (Malenovský *et al.*, 2009), and whether they are meaningful to spatiotemporal scales of remote sensing (i.e. seasonal scale, and canopy/landscape level with multiple species). In particular, the temporal variation of leaf-level traits discussed above (Section 5.1), the vertical variation in leaf-level traits such as leaf absorptance (Ellsworth and Reich, 1993), PSII:PSI stoichiometry, and relative absorption cross-sections (Chow *et al.*, 1990; Rivadossi *et al.*, 1999) observed within a plant canopy, and the variation of leaf-level traits across species, need to be characterized and implemented within these models.

5.3 Mechanistic up-scaling: from SIF to GPP

Despite the complexity of the relationship between SIF and GPP, and despite the limited spatial and temporal resolution of the currently available remotely sensed SIF data (10 km, monthly) the resemblance of global maps of satellite-retrieved SIF and modelled GPP (Frankenberg *et al.*, 2011; Joiner *et al.*, 2011; Guanter *et al.*, 2012) shows that the relationship between satellite-derived SIF and GPP is significant, albeit probably biome dependent. The question remains of whether we have enough process understanding to explain the correlation between SIF and GPP mechanistically. How can we assimilate SIF into models to improve/benchmark spatially distributed GPP estimates? The current practice of estimating GPP from remote sensing is to parameterize LUE (Equation 1) by means of either statistical (Xiao *et al.*, 2004; Jung *et al.*, 2011) or physically based models (e.g. Ryu *et al.*, 2011). In both approaches, a combination of flux tower data and remote sensing products are used.

An important question when considering Equation 1 is whether SIF can be used to infer LUE, APAR (where APAR=PAR×*f*APAR), or both. Remote sensing of green *f*APAR based on reflectance measurements remains a challenge due to signal saturation, bidirectional reflectance distribution function (BRDF) effects (Morton *et al.*, 2014), and because materials such as soil, wood, and dead biomass also absorb PAR but do not contribute to photosynthesis (Huete, 1988; Qi *et al.*, 1994; Daughtry *et al.*, 2000; Haboudane *et al.*, 2002). In contrast, because ChlF originates only from chlorophyll, SIF could improve the estimation of *f*APAR in comparison with current reflectance-based methods (Frankenberg *et al.*, 2011).

The question of whether SIF is a measure for LUE is difficult to answer. In contrast to PAM measurements, it is not obvious how SIF (Equation 20) can be related to photochemistry. The information in a measurement of SIF is simply insufficient to calculate the quantum yield of photochemistry as derived from Equation 9 (unknown F_m' when measuring SIF). The accumulated knowledge provided by PAM fluorescence measurements may provide a path to understanding and modelling the relationship between SIF, electron transport, and GPP.

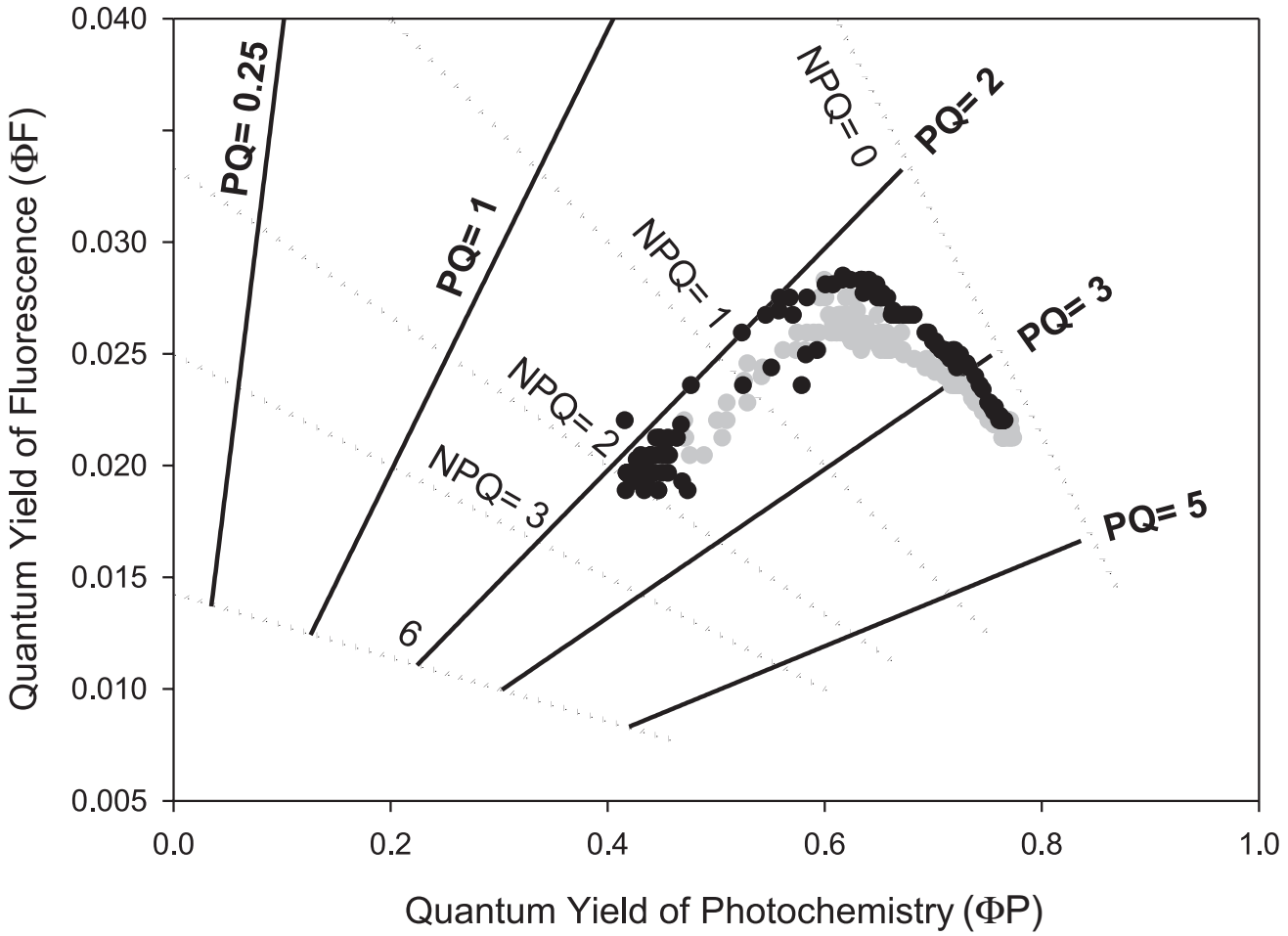

Fig. 9. Relationships between the quantum yields of photochemistry (ΦP) and fluorescence (ΦF) in relation to photochemical (PQ) and non-photochemical quenching (NPQ) of excitation energy. Lines were obtained by assuming a maximum quantum yield of fluorescence at the F_M state of 10% [i.e. k_F=0.1(k_F+k_D)], and by varying PQ and NPQ to estimate ΦF=0.1/(1+PQ+NPQ) and ΦP=PQ/(1+PQ+NPQ). It can be appreciated that under constant NPQ (dotted lines), fluorescence and photochemical yield are inversely proportional, whereas at constant PQ (solid lines), fluorescence and photochemical yield become proportional. Data were obtained during a summer day and using a Monitoring PAM fluorometer (Walz GmbH, Germany); data are from Porcar-Castell *et al.* (2008*c*). Black points correspond to data from midnight to noon, grey points from noon to midnight.

Fluorescence (ΦF) and photochemical (ΦP) yields (Equations 7 and 9, respectively) are affected by photochemical (PQ) and non-photochemical quenching (NPQ) (see Equation 10 and Fig. 9). In the field, the quantum yield of fluorescence is highly dynamic, both during the course of a day (Porcar-Castell *et al.*, 2008*b*) and throughout seasons (Soukupová *et al.*, 2008; Porcar-Castell, 2011), where ΦF decreases during stress episodes and increases upon recovery in a process that appears to be largely controlled by the presence of sustained NPQ forms (Ensminger *et al.*, 2004; Porcar-Castell *et al.*, 2008*a*; Porcar-Castell, 2011). Therefore, ΦF is related to ΦP and hence to LUE. In conclusion, SIF contains information relating to LUE as well as APAR. Yet, disentangling these two contributions remains a challenge from a remotely sensed large-scale observation platform.

Over the course of a day, the relationship between ΦF and ΦP falls apart into two distinct phases: under low light (first morning hours and towards sunset) the changes in the quantum yield of photochemistry are controlled by PQ, with NPQ remaining approximately constant and low (Fig. 9). In contrast, under high light (noon hours) the changes in ΦP are dominated by NPQ, with PQ remaining rather constant. Since decreasing PQ and increasing NPQ have opposite effects on ΦF (see Equation 7), this non-complementary behaviour generates a two-phased inverted 'V' relationship between ΦP and ΦF (Fig. 9), where ΦP and ΦF are inversely proportional under low light 'PQ-Phase', and proportional under high light 'NPQ-Phase'. The inverted 'V' relationship can be reproduced using current process-based understanding of the relationship between ChlF and photosynthesis (see Fig. 2 in van der Tol *et al.*, 2009).

Remotely sensed SIF will always be obtained under high-light conditions ('NPQ-Phase'); therefore, it could be expected that SIF and ΦP vary concomitantly in response to stress, with SIF~ΦF APAR. Indeed, a good correlation between ΦF and photosynthesis has been observed in response to water stress episodes (Flexas *et al.*, 2000) when measured under high light in the 'NPQ-Phase'. Similarly, both ΦF and ΦP tend to decrease simultaneously in response

to low temperatures due to the action of sustained NPQ (Soukupová *et al.*, 2008; Porcar-Castell, 2011). As a caveat, it is likely that the sensitivity of the relationship changes during the season in response to sustained NPQ or photoinhibition of reaction centres, something that remains to be clarified and awaits validation. For example, the hysteresis observed in Fig. 9 between morning and afternoon observations may indicate that these processes already play a role at the diurnal scale. Overall, the general relationship between ΦP and ΦF presented in Fig. 9 demonstrates the strong control of the fluorescence signal by the dynamics of PQ and NPQ. This link has been described with empirical relationships that have been parameterized in radiative transfer models (Lee *et al.*, 2013).

To understand further how ΦF and ΦP, as well as ΦF and SIF, are related at the seasonal scale, the following points need consideration. (i) Over the short term, NPQ is known to decrease both SIF and F', although for SIF the effect is known to be stronger when estimated in the red region (e.g. SIF_{690}) compared with the far-red (e.g. SIF_{760}) (Lichtenthaler and Rinderle, 1988; Agati *et al.*, 1995), most probably due to the NPQ-insensitive contribution of PSI far-red fluorescence. At the seasonal scale, the PAM term F' may decrease in response to stress due to accumulation of sustained forms of NPQ, yet, because stress is often accompanied by a decrease in chlorophyll content (i.e. decreased fluorescence reabsorption), SIF_{690} (retrieved in the red region) may actually increase instead of decreasing like F'. (ii) Similarly, seasonal changes in the contribution of PSI may equally interact with the expected relationship between ΦF and ΦP when using SIF_{760} (retrieved in the far-red) instead. Further long-term experimental work is needed to characterize the processes that control the relationship between $SIF_{\lambda retrieval}$, F', ΦF, and ΦP at the seasonal scale. Last, but not least, the seasonal dynamics of alternative electron sinks, alternative metabolic pathways, and photorespiration (Fig. 1) will need characterization before we can mechanistically link SIF and GPP.

6. Concluding remarks

The availability, quality, and spatiotemporal coverage of SIF data are expected to increase drastically over the next few years. At the canopy scale, field spectroradiometer prototype systems are being rapidly developed and deployed in increasing numbers (Rossini *et al.*, 2010; Balzarolo *et al.*, 2011; Drolet *et al.*, 2014). These systems will promote the expansion of SIF measurements at the ecosystem scale. The increased knowledge will hopefully lead to a better understanding of the SIF signal and its relationship to GPP. In addition, airborne instruments specifically designed to map vegetation fluorescence have recently been developed (Rascher *et al.*, 2009; Zarco-Tejada *et al.*, 2009, 2012). This opens the way for extensive airborne campaigns to better understand the significance of spatial variability in the SIF signal and facilitate the up-scaling from the canopy to the landscape levels. Finally, and most significantly, imminent space missions will herald a new range of possibilities for retrieving SIF at the global scale. This could result in improved estimates of the global carbon budget and our capacity to track the health of terrestrial ecosystems. In particular, the ESA's Earth Explorer Fluorescence Explorer (FLEX) (Moreno *et al.*, 2006; Kraft *et al.*, 2013) is expected to provide an unprecedented source of spatially continuous SIF data as well as other critical variables to facilitate the signal interpretation (e.g. photochemical reflectance index, canopy temperature, *f*APAR). Likewise, satellite missions such as the NASA OCO-2 (Frankenberg *et al.*, 2014) or the ESA Sentinels 4–5, sensors conceived to measure atmospheric properties, will also offer exciting possibilities to retrieve SIF. Despite this promising scenario and despite the empirical evidence that confirms that SIF carries novel information on the dynamics of photosynthesis compared with previous remote sensing data (Frankenberg *et al.*, 2011; Joiner *et al.*, 2011; Guanter *et al.*, 2012), the mechanistic link between SIF and GPP still remains unclear.

In this review, we identified a number of areas where further research is deemed necessary to understand fully the mechanisms that control the seasonality of the SIF signal at the leaf level. Three prospective research areas for future work can be summarized.

(i) Characterization of processes that uncouple ChlF and GPP at the seasonal scale. The seasonal variation of processes such as photosynthetic light absorption, CET, adjustments in relative absorption cross-sections of PSII and PSI, alternative sinks, PSI fluorescence contribution, photorespiration, photosystem connectivity, and the thermodynamic effect of temperature need to be characterized in order to understand and mechanistically model the seasonal link between ChlF and photosynthesis.

(ii) Linking PAM and SIF fluorescence at the seasonal scale. Combined measurements of PAM and spectrally resolved ChlF are needed at the seasonal and leaf scales to elucidate how the methodology affects the information content of the signal.

(iii) Characterizing the vertical and genetic variation in physiological traits. The variation in factors listed in (i) and (ii) within a plant canopy and across species still needs to be characterized fully in order to identify possible generic functions that could be implemented when upscaling from the leaf to the canopy and landscape levels.

Acknowledgements

This work has been supported by the Academy of Finland [grant nos 1138884 and 272041 to AP-C and 259075 to ET], and the University of Helsinki (grant no 490116). This review idea originated from discussions during a Workshop organized by the Keck Institute for Space Studies 'New Methods for Measurements of Photosynthesis from Space'. The availability of results from ongoing preparatory studies for the ESA FLEX mission is acknowledged. We thank Professor Kari Heliovaara for help in preparing Figs 2, 4, and 7.

Appendix 1. Interaction between PSII connectivity, fraction of open reaction centres *q*, and parameters *q*L and *q*P in the presence of NPQ. An analysis based on equations derived by Lavergne and Trissl, (1995)

Adaptation of the fluorescence yield equation as a function of q *for a connected units model*

We define a system with two populations of PSII units, open ($PSII_{open}$) and closed ($PSII_{closed}$). We assume rapid energy equilibration between peripheral antenna, core, and reaction centre (single pool model). We define 'q' as the fraction of PSII units with an open reaction centre. k_{LII} is the sum of rate constants of all non-photochemical quenching processes operating in the photosynthetic antenna, namely constitutive thermal dissipation, fluorescence, and regulated thermal energy dissipation (NPQ), $k_{LII}=k_D+k_F+k_{NPQ}$. We assume that thermal dissipation by open reaction centres, intersystem crossing, photobleaching, and spillover are insignificant and are embedded in k_D. Finally, k_{PSII} is the intrinsic rate constant of photochemistry in open reaction centres, and k_{CII} is the rate constant of energy transfer between photosynthetic units (Fig. A1).

According to the above system, three different connectivity models can be defined (Lavergne and Trissl, 1995): (i) a lake model, when k_{CII} tends to infinity; (ii) a separate units model, when k_{CII} tends to zero; and (iii) a connected units model when $0<k_{CII}<\infty$. We then redefine the parameters J, B, and C derived for a connected units model by Lavergne and Trissl (1995) using our nomenclature, where $k_{PSII}\equiv\alpha_P$ (therein), $k_{LII}\equiv k_l$ (therein), $k_{CII}\equiv k_{UU}$ (therein), $k_{RCII}\equiv\beta$ (therein), and $k_F\equiv k_{rad}$ (therein). Similarly, the rate constants k_{20} and k_{30} in Lavergne and Trissl (1995) are reformulated as (note that α_d, the rate constant of thermal dissipation by open centres, is assumed to be zero):

$$k_{20} = k_{PSII} + k_L \tag{A1}$$

$$k_{30} = k_{RCII} + k_L \tag{A2}$$

and the factors J, B, and C in Lavergne and Trissl (1995) become:

$$J = \frac{k_{CII}\left(k_{20}-k_{30}\right)}{k_{30}\left(k_{CII}+k_{20}\right)} = \frac{k_{CII}\left(k_{PSII}-k_{RCII}\right)}{\left(k_{RCII}+k_{LII}\right)\left(k_{CII}+k_{PSII}+k_{LII}\right)} \tag{A3}$$

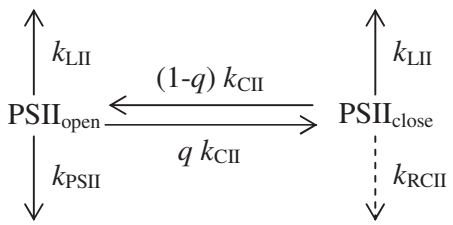

Figure A1. Schematic diagram indicating the main energy pathways in a system with open and closed populations of PSII units.

$$B = \frac{k_F}{k_{30}} = \frac{k_F}{k_{RCII}+k_{LII}} \tag{A4}$$

$$C = \frac{k_F\left(k_{30}-k_{20}\right)}{k_{30}\left(k_{CII}+k_{20}\right)} = -\frac{k_F\left(k_{PSII}-k_{RCII}\right)}{\left(k_{RCII}+k_{LII}\right)\left(k_{CII}+k_{PSII}+k_{LII}\right)} \tag{A5}$$

Subsequetly, using Equation 6*b* in Lavergne and Trissl (1995) to express the fluorescence yield as a function of q, we obtain:

$$\Phi F(q) = \frac{B+Cq}{1+Jq} = \frac{\dfrac{k_F}{k_{RCII}+k_{LII}} - \dfrac{k_F\left(k_{PSII}-k_{RCII}\right)}{\left(k_{RCII}+k_{LII}\right)\left(k_{CII}+k_{PSII}+k_{LII}\right)}q}{1+\dfrac{k_{CII}\left(k_{PSII}-k_{RCII}\right)}{\left(k_{RCII}+k_{LII}\right)\left(k_{CII}+k_{PSII}+k_{LII}\right)}q} \tag{A6}$$

and rearranging,

$$\Phi F(q) = \frac{\dfrac{k_F}{k_{RCII}+k_{LII}}\left(1-\dfrac{k_{PSII}-k_{RCII}}{k_{CII}+k_{PSII}+k_{LII}}q\right)}{\dfrac{k_{RCII}+k_{LII}}{k_{RCII}+k_{LII}}+\dfrac{k_{CII}\left(k_{PSII}-k_{RCII}\right)}{\left(k_{RCII}+k_{LII}\right)\left(k_{CII}+k_{PSII}+k_{LII}\right)}q} = \frac{k_F\left(1-\dfrac{k_{PSII}-k_{RCII}}{k_{CII}+k_{PSII}+k_{LII}}q\right)}{k_{RCII}+k_{LII}+\dfrac{k_{PSII}-k_{RCII}}{k_{CII}+k_{PSII}+k_{LII}}q\,k_{CII}} \tag{A7}$$

Finally, since the rate constant of thermal energy dissipation by closed PSII centres (with $P680^+$) (k_{RCII}) is only relevant for the interpretation of fluorescence data obtained with intense laser sources, we can assume that k_{RCII} equals zero and Equation A7 becomes:

$$\Phi F(q) = \frac{k_F\left(1-\dfrac{k_{PSII}}{k_{CII}+k_{PSII}+k_{LII}}q\right)}{k_{LII}+\dfrac{k_{PSII}}{k_{CII}+k_{PSII}+k_{LII}}q\,k_{CII}} \tag{A8}$$

Equation A8 was used to estimate F and F_M in Fig. 5, using parameter values reported in Lavergne and Trissl (1995) (Table A1), and adjusting k_{CII} and k_{LII} to represent different levels of connectivity and NPQ, respectively. For example, k_{LII}=0.3 ns^{-1} (NPQ=0), but becomes 0.6 ns^{-1} or 0.9 ns^{-1} if NPQ=1 or 2, respectively, as $NPQ=k_{NPQ}/(k_F+k_D)$.

Table 1A. *Parameter values*

Parameter	Correspondence in Lavergne and Trissl	Value (ns^{-1})
k_{PSII}	α_P	2.654
k_F	k_{rad}	0.056
k_{LII}	k_l	0.300

Demonstration of qL and qP

When k_{CII} approaches infinity (i.e. a lake model), Equation A8 becomes:

$$\Phi F(q)_{\text{Lake}} = \frac{k_F}{k_{LII} + q\,k_{PSII}} = \frac{k_F}{k_D + k_F + k_{NPQ} + q\,k_{PSII}} \quad \text{(A9)}$$

which is equivalent to Equation 7, demonstrating that qL is equal to q when connectivity approaches infinity. Conversely, if k_{CII} approaches zero (separate units model), and given that the sum of all quantum yields is by definition equal to unity, then

$$1 - \frac{k_{PSII}}{k_{PSII} + k_{LII}} = \frac{k_{LII}}{k_{PSII} + k_{LII}}, \quad \text{(A10)}$$

and we can express Equation A8 as:

$$\begin{aligned}
\Phi F(q)_{\text{SeparateUnits}} &= \frac{k_F\left(1 - \frac{k_{PSII}}{k_{PSII} + k_{LII}}q\right)}{k_{LII}} = \\
&\frac{k_F}{k_{LII}} - \frac{k_F\,k_{PSII}\,q}{k_{LII}(k_{PSII} + k_{LII})} = \\
&= (1-q)\frac{k_F}{k_{LII}} + q\frac{k_F}{k_{LII}} - \frac{k_F\,k_{PSII}\,q}{k_{LII}(k_{PSII} + k_{LII})} = \\
&(1-q)\frac{k_F}{k_{LII}} + q\left(\frac{k_F}{k_{LII}} - \frac{k_F\,k_{PSII}}{k_{LII}(k_{PSII} + k_{LII})}\right) = \\
&= (1-q)\frac{k_F}{k_{LII}} + q\frac{k_F}{k_{LII}}\left(1 - \frac{k_{PSII}}{k_{PSII} + k_{LII}}\right) = \\
&(1-q)\frac{k_F}{k_{LII}} + q\frac{k_F}{k_{LII}}\frac{k_{LII}}{(k_{PSII} + k_{LII})} = \\
&(1-q)\frac{k_F}{k_{LII}} + q\frac{k_F}{k_{PSII} + k_{LII}}
\end{aligned} \quad \text{(A11)}$$

which is equivalent to the separate units formulation of q, that corresponds to the parameter qP (Genty *et al.* 1989). The performance of qL and qP under intermediate connectivity scenarios and in the presence of NPQ is assessed in Fig. 5.

References

Adams WW III, Demmig-Adams B. 1994. Carotenoid composition and down regulation of Photosystem II in three conifer species during the winter. *Physiologia Plantarum* **92,** 451–458.

Adams WW III, Demmig-Adams B. 2004. Chlorophyll fluorescence as a tool to monitor plant response to the environment. In: Papageorgiou GC, Govindjee, eds. *Chlorophyll a fluorescence, a signature of photosynthesis. Advances in Photosynthesis and Respiration* , Vol. **19**. Dordrecht: Springer, 583–604.

Adams WW III, Winter K, Schreiber U, Schramel P. 1990. Photosynthesis and chlorophyll fluorescence characteristics in relationship to changes in pigment and element composition of leaves of *Platanus occidentalis* L. during autumnal leaf senescence. *Plant Physiology* **92,** 1184–1190.

Agati G. 1998. Response of the *in vivo* chlorophyll fluorescence spectrum to environmental factors and laser excitation wavelength. *Pure and Applied Optics* **7,** 797–807.

Agati G, Cerovic ZG, Moya I. 2000. The effect of decreasing temperature up to chilling values on the *in vivo* F685/F735 chlorophyll fluorescence ratio in *Phaseolus vulgaris* and *Pisum sativum*: the role of the photosystem I contribution to the 735 nm fluorescence band. *Photochemistry and Photobiology* **72,** 75–84.

Agati G, Mazzinghi P, Fusi F, Ambrosini I. 1995. The F685/F730 chlorophyll fluorescence ratio as a tool in plant physiology: response to physiological and environmental factors. *Journal of Plant Physiology* **145,** 228–238.

Allen E. 1964. Fluorescent white dyes: calculation of fluorescence from reflectivity values. *Journal of the Optical Society of America* **54,** 506–514.

Anderson JM, Chow WS, Goodchild DJ. 1988. Thylakoid membrane organisation in sun/shade acclimation. *Australian Journal of Plant Physiology* **15,** 11–26.

Andrizhiyevskaya EG, Frolov D, van Grondelle R, Dekker JP. 2004. On the role of the CP47 core antenna in the energy transfer and trapping dynamics of photosystem II. *Physical Chemistry Chemical Physics* **6,** 4810–4819.

Antal TK, Kovalenko IB, Rubin AB, Tyystjärvi E. 2013. Photosynthesis-related quantities for education and modeling. *Photosynthesis Research* **117,** 1–30.

Arena C, Vitale L, De Santo AV. 2008. Paraheliotropism in *Robinia pseudoacacia* L.: an efficient strategy to optimise photosynthetic performance under natural environmental conditions. *Plant Biology* **10,** 194–201.

Asada K. 2000. The water–water cycle as alternative photon and electron sinks. *Philosophical Transactions of the Royal Society B: Biological Sciences* **355,** 1419–1431.

Atkin OK, Bruhn D, Hurry VM, Tjoelker MG. 2005. Evans Review No. 2. The hot and the cold: unravelling the variable response of plant respiration to temperature. *Functional Plant Biology* **32,** 87–105.

Baker NR. 2008. Chlorophyll fluorescence: a probe of photosynthesis *in vivo*. *Annual Review of Plant Biology* **59,** 89–113.

Baker NR, Oxborough K. 2004. Chlorophyll fluorescence as a probe of photosynthetic productivity. In: Papageorgiou GC, Govindjee, eds. *Chlorophyll a fluorescence, a signature of photosynthesis. Advances in Photosynthesis and Respiration* , Vol. **19**. Dordrecht: Springer, 65–82.

Baldocchi D. 2008. Breathing of the terrestrial biosphere: lessons learned from a global network of carbon dioxide flux measurement systems. *Australian Journal of Botany* **56,** 1–26.

Ballottari M, Dall'Osto L, Morosinotto T, Bassi R. 2007. Contrasting behavior of higher plant photosystem I and II antenna systems during acclimation. *Journal of Biological Chemistry* **282,** 8947–8958.

Balzarolo M, Anderson K, Nichol C, *et al*. 2011. Ground-based optical measurements at European flux sites: a review of methods, instruments and current controversies. *Sensors* **11,** 7954–7981.

Barber J, Malkin S, Telfer A, Schreiber U. 1989. The origin of chlorophyll fluorescence *in vivo* and its quenching by the photosystem II reaction centre. *Philosophical Transactions of the Royal Society B: Biological Sciences* **323,** 227–239.

Barber J, Andersson B. 1992. Too much of a good thing: light can be bad for photosynthesis. *Trends in Biochemical Sciences* **17,** 61–66.

Barton CVM, North PRJ. 2001. Remote sensing of canopy light use efficiency using the photochemical reflectance index: model and sensitivity analysis. *Remote Sensing of Environment* **78,** 264–273.

Beer C, Reichstein M, Tomelleri E, *et al*. 2010. Terrestrial gross carbon dioxide uptake: global distribution and covariation with climate. *Science* **329,** 834–838.

Ben-Shem A, Frolow F, Nelson N. 2003. Crystal structure of plant photosystem I. *Nature* **426,** 630–635.

Biehler K, Fock H. 1996. Evidence for the contribution of the Mehler-peroxidase reaction in dissipating excess electrons in drought-stressed wheat. *Plant Physiology* **112,** 265–272.

Bilger W, Björkman O. 1991. Temperature dependence of violaxanthin de-epoxidation and non-photochemical fluorescence quenching in intact leaves of *Gossypium hirsutum* L. and *Malva parviflora* L. *Planta* **184,** 226–234.

Björkman O, Demmig B. 1987. Photon yield of O_2 evolution and chlorophyll fluorescence characteristics at 77 K among vascular plants of diverse origins. *Planta* **170,** 489–504.

Boichenko VA. 1998. Action spectra and functional antenna sizes of Photosystems I and II in relation to the thylakoid membrane organization and pigment composition. *Photosynthesis Research* **58,** 163–174.

Bolhàr-Nordenkampf HR, Long SP, Baker NR, Öquist G, Schreiber U, Lechner EG. 1989. Chlorophyll fluorescence as a probe of the photosynthetic competence of leaves in the field: a review of current instrumentation. *Functional Ecology* **3,** 497–514.

Bradbury M, Baker NR. 1981. Analysis of the slow phases of the *in vivo* chlorophyll fluorescence induction curve. Changes in the redox state of photosystem II electron acceptors and fluorescence emission from photosystems I and II. *Biochimica et Biophysica Acta* **635,** 542–551.

Britt RD. 1996. Oxygen evolution. In: Ort DR, Yocum CF, eds. *Oxygenic photosynthesis: the light reactions*. Dordrecht: Kluwer Academic Publishers, 137–164.

Brody SS, Brody M. 1962. Fluorescence properties of aggregated chlorophyll *in vivo* and *in vitro*. *Transactions of the Faraday Society* **58,** 416–428.

Brody SS, Rabinowitch E. 1957. Excitation lifetime of photosynthetic pigments *in vitro* and *in vivo*. *Science* **125,** 555–557.

Brugnoli E, Björkman O. 1992. Chloroplast movements in leaves: influence on chlorophyll fluorescence and measurements of light-induced absorbance changes related to ΔpH and zeaxanthin formation. *Photosynthesis Research* **32,** 23–35.

Buschmann C, Lichtenthaler HK. 1998. Principles and characteristics of multi-colour fluorescence imaging of plants. *Journal of Plant Physiology* **152,** 297–314.

Butler WL. 1978. Energy distribution in the photochemical apparatus of photosynthesis. *Annual Review of Plant Physiology* **29,** 345–378.

Butler WL, Kitajima M. 1975. Fluorescence quenching in photosystem II of chloroplasts. *Biochimica et Biophysica Acta* **376,** 116–125.

Campbell DA, Tyystjärvi E. 2012. Parameterization of photosystem II photoinactivation and repair. *Biochimica et Biophysica Acta* **1817,** 258–265.

Campbell PE, Middleton E, Corp L, Kim M. 2008. Contribution of chlorophyll fluorescence to the apparent vegetation reflectance. *Science of the Total Environment* **404,** 433–439.

Chow WS, Kim E, Horton P, Anderson JM. 2005. Granal stacking of thylakoid membranes in higher plant chloroplasts: the physicochemical forces at work and the functional consequences that ensue. *Photochemical and Photobiological Sciences* **4,** 1081–1090.

Chow WS, Melis A, Anderson JM. 1990. Adjustments of photosystem stoichiometry in chloroplasts improve the quantum efficiency of photosynthesis. *Proceedings of the National Academy of Sciences, USA* **87,** 7502–7506.

Clegg RM. 2004. Nuts and bolts of excitation energy migration and energy transfer. In: Papageorgiou GC, Govindjee, eds. *Chlorophyll a fluorescence, a signature of photosynthesis. Advances in Photosynthesis and Respiration* , Vol. **19**. Dordrecht: Springer, 83–105.

Close DC, Beadle CL. 2003. The ecophysiology of foliar anthocyanin. *Botanical Review* **69,** 149–161.

Croce R, Zucchelli G, Garlaschi FM, Bassi R, Jennings RC. 1996. Excited state equilibration in the photosystem I-light-harvesting I complex: P700 is almost isoenergetic with its antenna. *Biochemistry* **35,** 8572–8579.

Dau H. 1994. Molecular mechanisms and quantitative models of variable photosystem II fluorescence. *Photochemistry and Photobiology* **60,** 1–23.

Dau H, Sauer K. 1996. Exciton equilibration and photosystem II exciton dynamics—a fluorescence study on photosystem II membrane particles of spinach. *Biochimica et Biophysica Acta* **1273,** 175–190.

Daughtry CST, Walthall CL, Kim MS, De Colstoun EB, McMurtrey JE III. 2000. Estimating corn leaf chlorophyll concentration from leaf and canopy reflectance. *Remote Sensing of Environment* **74,** 229–239.

Daumard F, Goulas Y, Champagne S, Fournier A, Ounis A, Olioso A, Moya I. 2012. Continuous monitoring of canopy level sun-induced chlorophyll fluorescence during the growth of a sorghum field. *IEEE Transactions on Geoscience and Remote Sensing* **50,** 4292–4300.

Demmig-Adams B. 1990. Carotenoids and photoprotection in plants: a role for the xanthophyll zeaxanthin. *Biochimica et Biophysica Acta* **1020,** 1–24.

Demmig-Adams B. 1998. Survey of thermal energy dissipation and pigment composition in sun and shade leaves. *Plant and Cell Physiology* **39,** 474–482.

Demmig-Adams B, Adams WW III. 2000. Harvesting sunlight safely. *Nature* **403,** 371–374.

Demmig-Adams B, Adams WW III. 2006. Photoprotection in an ecological context: the remarkable complexity of thermal energy dissipation. *New Phytologist* **172,** 11–21.

Diaz M, de Haro V, Munoz R, Quiles MJ. 2007. Chlororespiration is involved in the adaptation of *Brassica* plants to heat and high light intensity. *Plant, Cell and Environment* **30,** 1578–1585.

Drolet GG, Huemmrich KF, Hall FG, Middleton EM, Black TA, Barr AG, Margolis HA. 2005. A MODIS-derived photochemical reflectance index to detect inter-annual variations in the photosynthetic light-use efficiency of a boreal deciduous forest. *Remote Sensing of Environment* **98,** 212–224.

Drolet GG, Wade T, Nichol CJ, MacLellan C, Levula J, Porcar-Castell A, Nikinmaa E, Vesala T. 2014. A temperature-controlled spectrometer system for continuous and unattended measurements of canopy spectral radiance and reflectance. *International Journal of Remote Sensing* **35,** 1769–1785.

Durnford DG, Falkowski PG. 1997. Chloroplast redox regulation of nuclear gene transcription during photoacclimation. *Photosynthesis Research* **53,** 229–241.

Duysens LNM. 1979. Transfer and trapping of excitation energy in photosystem II. In: Wolstenholme GEW, Fitssimons DW, eds. *Chlorophyll organization and energy transfer in photosynthesis. CIBA Foundation Symposium* , Vol. **61**. Amsterdam: Exerpta Medica, 323–364.

Duysens LNM, Sweers HE. 1963. Mechanism of two photochemical reactions in algae as studied by means of fluorescence. In: *Japanese Society of Plant Physiologists* , eds. *Studies on microalgae and photosynthetic bacteria*. Tokyo: University of Tokyo Press, 353–372.

Ehleringer J, Bjorkman O, Mooney HA. 1976. Leaf pubescence: effects on absorptance and photosynthesis in a desert shrub. *Science* **192,** 376–377.

Eichelmann H, Oja V, Rasulov B, Padu E, Bichele I, Pettai H, Mänd P, Kull O, Laisk A. 2005. Adjustment of leaf photosynthesis to shade in a natural canopy: reallocation of nitrogen. *Plant, Cell and Environment* **28,** 389–401.

Ellsworth D, Reich P. 1993. Canopy structure and vertical patterns of photosynthesis and related leaf traits in a deciduous forest. *Oecologia* **96,** 169–178.

Engel GS, Calhoun TR, Read EL, Ahn T-K, Mančal T, Cheng Y-C, Blankenship RE, Fleming GR. 2007. Evidence for wavelike energy transfer through quantum coherence in photosynthetic systems. *Nature* **446,** 782–786.

Ensminger I, Busch F, Huner NPA. 2006. Photostasis and cold acclimation: sensing low temperature through photosynthesis. *Physiologia Plantarum* **126,** 28–44.

Ensminger I, Sveshnikov D, Campbell DA, Funk C, Jansson S, Lloyd J, Shibistova O, Öquist G. 2004. Intermittent low temperatures constrain spring recovery of photosynthesis in boreal Scots pine forests. *Global Change Biology* **10,** 995–1008.

Eskling M, Arvidsson P, Åkerlund H-E. 1997. The xanthophyll cycle, its regulation and components. *Physiologia Plantarum* **100,** 806–816.

Esteban R, Fernández-Marín B, Hernandez A, *et al*. 2013. Salt crystal deposition as a reversible mechanism to enhance photoprotection in black mangrove. *Trees* **27,** 229–237.

Evain S, Flexas J, Moya I. 2004. A new instrument for passive remote sensing: 2. Measurement of leaf and canopy reflectance changes at 531 nm and their relationship with photosynthesis and chlorophyll fluorescence. *Remote Sensing of Environment* **91,** 175–185.

Färber A, Young AJ, Ruban AV, Horton P, Jahns P. 1997. Dynamics of xanthophyll-cycle activity in different antenna subcomplexes in the photosynthetic membranes of higher plants: the relationship between zeaxanthin conversion and nonphotochemical fluorescence quenching. *Plant Physiology* **115,** 1609–1618.

Filella I, Porcar-Castell A, Munné-Bosch S, Bäck J, Garbulsky M, Peñuelas J. 2009. PRI assessment of long-term changes in carotenoids/chlorophyll ratio and short-term changes in de-epoxidation state of the xanthophyll cycle. *International Journal of Remote Sensing* **30,** 4443–4455.

Flexas J, Badger M, Chow WS, Medrano H, Osmond CB. 1999. Analysis of the relative increase in photosynthetic O(2) uptake when photosynthesis in grapevine leaves is inhibited following low night temperatures and/or water stress. *Plant Physiology* **121,** 675–684.

Flexas J, Briantais J-M, Cerovic Z, Medrano H, Moya I. 2000. Steady-state and maximum chlorophyll fluorescence responses to water stress in grapevine leaves: a new remote sensing system. *Remote Sensing of Environment* **73,** 283–297.

Flexas J, Galmes J, Ribas-Carbo M, Medrano H. 2005. The effects of water stress on plant respiration. In: Lambers H, Ribas-Carbó M, eds. *Plant respiration: from cell to ecosystem. Advances in Photosynthesis and Respiration* , Vol. **18**. Dordrecht: Springer, 85–94.

Flexas J, Medrano H. 2002. Energy dissipation in C3 plants under drought. *Functional Plant Biology* **29,** 1209–1215.

Franck F, Juneau P, Popovic R. 2002. Resolution of the photosystem I and photosystem II contributions to chlorophyll fluorescence of intact leaves at room temperature. *Biochimica et Biophysica Acta* **1556,** 239–246.

Frankenberg C, Fisher JB, Worden J, *et al*. 2011. New global observations of the terrestrial carbon cycle from GOSAT: patterns of plant fluorescence with gross primary productivity. *Geophysical Research Letters* **38,** L17706.

Frankenberg C, O'Dell C, Berry JA, Guanter L, Joiner J, Köhler P, Pollock R, Taylor TE. 2014. Prospects for chlorophyll fluorescence remote sensing from the Orbiting Carbon Observatory-2. *Remote Sensing of Environment* **147,** 1–12.

Freedman A, Cavender-Bares J, Kebabian P, Bhaskar R, Scott H, Bazzaz FA. 2002. Remote sensing of solar-excited plant fluorescence as a measure of photosynthetic rate. *Photosynthetica* **40,** 127–132.

Galmés J, Medrano H, Flexas J. 2007*a*. Photosynthesis and photoinhibition in response to drought in a pubescent (var. *minor*) and a glabrous (var. *palaui*) variety of *Digitalis minor*. *Environmental and Experimental Botany* **60,** 105–111.

Galmés J, Ribas-Carbó M, Medrano H, Flexas J. 2007*b*. Response of leaf respiration to water stress in Mediterranean species with different growth forms. *Journal of Arid Environments* **68,** 206–222.

Gamon JA, Field CB, Bilger W, Björkman O, Fredeen AL, Peñuelas J. 1990. Remote sensing of the xanthophyll cycle and chlorophyll fluorescence in sunflower leaves and canopies. *Oecologia* **85,** 1–7.

Gamon JA, Penuelas J, Field CB. 1992. A narrow-waveband spectral index that tracks diurnal changes in photosynthetic efficiency. *Remote Sensing of Environment* **41,** 35–44.

Garbulsky MF, Peñuelas J, Papale D, Filella I. 2008. Remote estimation of carbon dioxide uptake by a Mediterranean forest. *Global Change Biology* **14,** 2860–2867.

García-Plazaola JI, Becerril JM. 2001. Seasonal changes in photosynthetic pigments and antioxidants in beech (*Fagus sylvatica*) in a Mediterranean climate: implications for tree decline diagnosis. *Australian Journal of Plant Physiology* **28,** 225–232.

García-Plazaola JI, Esteban R, Fernández-Marín B, Kranner I, Porcar-Castell A. 2012. Thermal energy dissipation and xanthophyll cycles beyond the Arabidopsis model. *Photosynthesis Research* **113,** 89–103.

Gastellu-Etchegorry J, Martin E, Gascon F. 2004. DART: a 3D model for simulating satellite images and studying surface radiation budget. *International Journal of Remote Sensing* **25,** 73–96.

Genty B, Briantais J-M, Baker NR. 1989. The relationship between the quantum yield of photosynthetic electron transport and quenching of chlorophyll fluorescence. *Biochimica et Biophysica Acta* **990,** 87–92.

Genty B, Harbinson J, Baker NR. 1990*a*. Relative quantum efficiencies of the two photosystems of leaves in photorespiratory and non-respiratory conditions. *Plant Physiology and Biochemistry (Paris)* **28,** 1–10.

Genty B, Wonders J, Baker NR. 1990*b*. Non-photochemical quenching of F_0 in leaves is emission wavelength dependent: consequences for quenching analysis and its interpretation. *Photosynthesis Research* **26,** 133–139.

Gillbro T, Cogdell RJ. 1989. Carotenoid fluorescence. *Chemical Physics Letters* **158,** 312–316.

Gilmore AM, Ball MC. 2000. Protection and storage of chlorophyll in overwintering evergreens. *Proceedings of the National Academy of Sciences, USA* **97,** 11098–11101.

Gilmore AM, Hazlett TL, Govindjee. 1995. Xanthophyll cycle-dependent quenching of photosystem II chlorophyll a fluorescence: formation of a quenching complex with a short fluorescence lifetime. *Proceedings of the National Academy of Sciences, USA* **92,** 2273–2277.

Gitelson AA, Buschmann C, Lichtenthaler HK. 1998. Leaf chlorophyll fluorescence corrected for re-absorption by means of absorption and reflectance measurements. *Journal of Plant Physiology* **152,** 283–296.

Gobets B, van Grondelle R. 2001. Energy transfer and trapping in photosystem I. *Biochimica et Biophysica Acta* **1507,** 80–99.

Goerner A, Reichstein M, Tomelleri E, Hanan N, Rambal S, Papale D, Dragoni D, Schmullius C. 2011. Remote sensing of ecosystem light use efficiency with MODIS-based PRI. *Biogeosciences* **8,** 189–202.

Goudriaan J. 1988. The bare bones of leaf-angle distribution in radiation models for canopy photosynthesis and energy exchange. *Agricultural and Forest Meteorology* **43,** 155–169.

Goulden ML, Munger JW, Fan S-M, Daube BC, Wofsy SC. 1996. Measurements of carbon sequestration by long-term eddy covariance: methods and a critical evaluation of accuracy. *Global Change Biology* **2,** 169–182.

Govindjee. 1995. Sixty-three years since Kautsky: chlorophyll-a fluorescence. *Australian Journal of Plant Physiology* **22,** 131–160.

Govindjee. 2004. Chlorophyll a fluorescence: a bit of basics and history. In: Papageorgiou GC, Govinjee, ed. *Chlorophyll a fluorescence, a signature of photosynthesis. Advances in Photosynthesis and Respiration* , Vol. **19**. Dordrecht: Springer, 1–42.

Govindjee, Yang L. 1966. Structure of the red fluorescence band in chloroplasts. *Journal of General Physiology* **49,** 763–780.

Grace J, Nichol C, Disney M, Lewis P, Quaife T, Bowyer P. 2007. Can we measure terrestrial photosynthesis from space directly, using spectral reflectance and fluorescence? *Global Change Biology* **13,** 1484–1497.

Greer DH, Berry JA, Björkman O. 1986. Photoinhibition of photosynthesis in intact bean leaves: role of light and temperature, and requirement for chloroplast-protein synthesis during recovery. *Planta* **168,** 253–260.

Guanter L, Alonso L, Gómez-Chova L, Amorós-López J, Vila J, Moreno J. 2007. Estimation of solar-induced vegetation fluorescence from space measurements. *Geophysical Research Letters* **34,** L08401.

Guanter L, Frankenberg C, Dudhia A, Lewis PE, Gómez-Dans J, Kuze A, Suto H, Grainger RG. 2012. Retrieval and global assessment of terrestrial chlorophyll fluorescence from GOSAT space measurements. *Remote Sensing of Environment* **121,** 236–251.

Guanter L, Rossini M, Colombo R, Meroni M, Frankenberg C, Lee JL, Joiner J. 2013. Using field spectroscopy to assess the potential of statistical approaches for the retrieval of sun-induced chlorophyll fluorescence from ground and space. *Remote Sensing of Environment* **133,** 52–61.

Gylle MA, Rantamäki S, Ekelund NGA, Tyystjärvi E. 2012. Fluorescence emission spectra of marine and brackish-water ecotypes of *Fucus vesiculosus* and *Fucus radicans* (Phaeophyceae) reveal differences in light-harvesting apparatus. *Photochemistry and Photobiology* **88,** 1455–1460.

Haboudane D, Miller JR, Tremblay N, Zarco-Tejada PJ, Dextraze L. 2002. Integrated narrow-band vegetation indices for prediction of crop chlorophyll content for application to precision agriculture. *Remote Sensing of Environment* **81,** 416–426.

Haldrup A, Jensen PE, Lunde C, Scheller HV. 2001. Balance of power: a view of the mechanism of photosynthetic state transitions. *Trends in Plant Science* **6,** 301–305.

Hatch MD. 1992. C_4 photosynthesis: an unlikely process full of surprises. *Plant and Cell Physiology* **33,** 333–342.

Havaux M, Strasser RJ, Greppin H. 1991. A theoretical and experimental analysis of the qP and qN coefficients of chlorophyll

fluorescence quenching and their relation to photochemical and nonphotochemical events. *Photosynthesis Research* **27,** 41–55.

Heinsch FA, Zhao M, Running SW, *et al*. 2006. Evaluation of remote sensing based terrestrial productivity from MODIS using regional tower eddy flux network observations. *IEEE Transactions on Geoscience and Remote Sensing* **44,** 1908–1925.

Hihara Y, Sonoike K. 2001. Regulation, inhibition and protection of photosystem I. In: Aro E-M, Andersson B. eds. *Regulation of photosynthesis*. Dordrecht: Kluwer Academic Publishers, 507–531.

Hilker T, Coops NC, Wulder MA, Black TA, Guy RD. 2008. The use of remote sensing in light use efficiency based models of gross primary production: a review of current status and future requirements. *Science of the Total Environment* **404,** 411–423.

Hlavinka J, Nauš J, Špundová M. 2013. Anthocyanin contribution to chlorophyll meter readings and its correction. *Photosynthesis Research* **118,** 277–295.

Hoff AJ. 1986. Triplets: phosphorescence and magnetic resonance. In: Govindjee, Amesz J, Fork DC, eds. *Light emission by plants and bacteria*. Orlando: Academic Press, 225–289.

Holt NE, Zigmantas D, Valkunas L, Li X-P, Niyogi KK, Fleming GR. 2005. Carotenoid cation formation and the regulation of photosynthetic light harvesting. *Science* **307,** 433–436.

Horton P, Hague A. 1988. Studies on the induction of chlorophyll fluorescence in isolated barley protoplasts. IV. Resolution of non-photochemical quenching. *Biochimica et Biophysica Acta* **932,** 107–115.

Horton P, Ruban AV, Walters RG. 1996. Regulation of light harvesting in green plants. *Annual Review of Plant Biology and Plant Molecular Biology* **47,** 655–684.

Huete A. 1988. A soil-adjusted vegetation index (SAVI). *Remote Sensing of Environment* **2,** 295–309.

Huete A, Liu H, Batchily K, Van Leeuwen W. 1997. A comparison of vegetation indices over a global set of TM images for EOS-MODIS. *Remote Sensing of Environment* **59,** 440–451.

Huner NPA, Maxwell DP, Gray GR, Savitch LV, Krol M, Ivanov AG, Falk S. 1996. Sensing environmental temperature change through imbalances between energy supply and energy consumption: redox state of photosystem II. *Physiologia Plantarum* **98,** 358–364.

Ilík P, Vystrčilová M, Nauš J, Kalina J. 1997. Chlorophyll fluorescence temperature curves of spruce needles from different whorls of the tree. *Photosynthetica* **34,** 477–480.

Ivanov AG, Sane PV, Hurry V, Öquist G, Huner NPA. 2008. Photosystem II reaction centre quenching: mechanisms and physiological role. *Photosynthesis Research* **98,** 565–574.

Ivanov AG, Sane PV, Zeinalov Y, Malmberg G, Gardeström P, Huner NPA, Öquist G. 2001. Photosynthetic electron transport adjustments in overwintering Scots pine (*Pinus sylvestris* L.). *Planta* **213,** 575–585.

Ivanov AG, Sane PV, Zeinalov Y, Simidjiev I, Huner NPA, Öquist G. 2002. Seasonal responses of photosynthetic electron transport in Scots pine (*Pinus sylvestris* L.) studied by thermoluminescence. *Planta* **215,** 457–465.

Jahns P, Holzwarth AR. 2012. The role of the xanthophyll cycle and of lutein in photoprotection of photosystem II. *Biochimica et Biophysica Acta* **1817,** 182–193.

Jennings RC, Zucchelli G, Croce R, Garlaschi FM. 2003. The photochemical trapping rate from red spectral states in PSI–LHCI is determined by thermal activation of energy transfer to bulk chlorophylls. *Biochimica et Biophysica Acta* **1557,** 91–98.

Joiner J, Guanter L, Lindstrot R, Voigt M, Vasilkov AP, Middleton EM, Huemmrich KF, Yoshida Y, Frankenberg C. 2013. Global monitoring of terrestrial chlorophyll fluorescence from moderate spectral resolution near-infrared satellite measurements: methodology, simulations, and application to GOME-2. *Atmospheric Measurement Techniques Discussions* **6,** 3883–3930.

Joiner J, Yoshida Y, Vasilkov AP, Yoshida Y, Corp LA, Middleton E. 2011. First observations of global and seasonal terrestrial chlorophyll fluorescence from space. *Biogeosciences* **8,** 637–651.

Joliot A, Joliot P. 1964. Etude cinétique de la réaction photochimique libérant l'oxygène au cours de la photosynthèse. *Comptes Rendus de l'Académie des Sciences* **258,** 4622–4625.

Joliot P, Joliot A. 2002. Cyclic electron transfer in plant leaf. *Proceedings of the National Academy of Sciences, USA* **99,** 10209–10214.

Jung M, Reichstein M, Margolis HA, *et al.* 2011. Global patterns of land–atmosphere fluxes of carbon dioxide, latent heat, and sensible heat derived from eddy covariance, satellite, and meteorological observations. *Journal of Geophysical Research G: Biogeosciences* **116,** G00J07.

Keränen M, Aro E-M, Tyystjärvi E. 1999. Excitation–emission map as a tool in studies of photosynthetic pigment–protein complexes. *Photosynthetica* **37,** 225–237.

Kitajima M, Butler WL. 1975*a*. Quenching of chlorophyll fluorescence and primary photochemistry in chloroplasts by dibromothymoquinone. *Biochimica et Biophysica Acta* **376,** 105–115.

Kitajima M, Butler WL. 1975*b*. Excitation spectra for photosystem I and photosystem II in chloroplasts and the spectral characteristics of the distribution of quanta between the two photosystems. *Biochimica et Biophysica Acta* **408,** 297–305.

Kok B. 1956. On the inhibition of photosynthesis by intense light. *Biochimica et Biophysica Acta* **21,** 234–244.

Kolari P, Lappalainen HK, Hänninen H, Hari P. 2007. Relationship between temperature and the seasonal course of photosynthesis in Scots pine at northern timberline and in southern boreal zone. *Tellus B* **59,** 542–552.

Kolber Z, Klimov D, Ananyev G, Rascher U, Berry J, Osmond B. 2005. Measuring photosynthetic parameters at a distance: laser induced fluorescence transient (LIFT) method for remote measurements of photosynthesis in terrestrial vegetation. *Photosynthesis Research* **84,** 121–129.

Kraft S, Del Bello U, Drusch M, Gabriele A, Harnisch B, Moreno J. 2013. On the demands on imaging spectrometry for the monitoring of global vegetation fluorescence from space. *SPIE Proceedings* **8870,** 88700N–12.

Krall JP, Edwards GE. 1992. Relationship between photosystem II activity and CO2 fixation in leaves. *Physiologia Plantarum* **86,** 180–187.

Kramer DM, Avenson TJ, Edwards GE. 2004*a*. Dynamic flexibility in the light reactions of photosynthesis governed by both electron and proton transfer reactions. *Trends in Plant Science* **9,** 349–357.

Kramer DM, Johnson G, Kiirats O, Edwards GE. 2004*b*. New fluorescence parameters for the determination of QA redox state and excitation energy fluxes. *Photosynthesis Research* **79,** 209–218.

Krause GH. 1988. Photoinhibition of photosynthesis. An evaluation of damaging and protective mechanisms. *Physiologia Plantarum* **74,** 566–574.

Krause GH, Jahns P. 2004. Non-photochemical energy dissipation determined by chlorophyll fluorescence quenching: characterization and function. In: Papageorgiou GC, Govindjee, eds. *Chlorophyll a fluorescence, a signature of photosynthesis. Advances in Photosynthesis and Respiration* , Vol. **19**. Dordrecht: Springer, 463–495.

Krause G, Weis E. 1991. Chlorophyll fluorescence and photosynthesis: the basics. *Annual Review of Plant Biology* **42,** 313–349.

Krivosheeva A, Tao D, Ottander C, Wingsle G, Dube SL, Öquist G. 1996. Cold acclimation and photoinhibition of photosynthesis in Scots pine. *Planta* **200,** 296–305.

Kumar M, Monteith JL. 1981. Remote sensing of crop growth. In: Smith H, ed. *Plants and the daylight spectrum*. London: Academic Press, 133–144.

Kuropatwa R, Naus J, Klinkovsky T, Ilik P, Kalina J, Maslan M, Zak D, Lattova J, Pavlova Z. 1992. The chlorophyll fluorescence temperature curve as a plant damage and light acclimation diagnostic tool. In: Murata N, ed. *Research in photosynthesis* , **Vol. 4**. Dordrecht: Kluwer Academic Publishers, 177–180.

Kyle DJ, Haworth P, Arntzen C. 1982. Thylakoid membrane protein phosphorylation leads to a decrease in connectivity between photosystem II reaction centers. *Biochimica et Biophysica Acta* **680,** 336–342.

Laisk A, Oja V, Rasulov B, Eichelmann H, Sumberg A. 1997. Quantum yields and rate constants of photochemical and nonphotochemical excitation quenching. Experiment and model. *Plant Physiology* **115,** 803–815.

Laisk A, Oja V, Rasulov B, Rämma H, Eichelmann H, Kasparova I, Pettai H, Padu E, Vapaavuori E. 2002. A computer-operated routine

of gas exchange and optical measurements to diagnose photosynthetic apparatus in leaves. *Plant, Cell and Environment* **25,** 923–943.

Latimer P, Bannister TT, Rabinowitch E. 1956. Quantum yields of fluorescence of plant pigments. *Science* **124,** 585–586.

Laureau C, de Paepe R, Latouche G, Moreno-Chacón M, Finazzi G, Kuntz M, Cornic G, Streb P. 2013. Plastid terminal oxidase (PTOX) has the potential to act as a safety valve for excess excitation energy in the alpine plant species *Ranunculus glacialis* L. *Plant, Cell and Environment* **36,** 1296–1310.

Lavergne J, Trissl H-W. 1995. Theory of fluorescence induction in photosystem II: derivation of analytical expressions in a model including exciton–radical-pair equilibrium and restricted energy transfer between photosynthetic units. *Biophysical Journal* **68,** 2474–2492.

Lazár D. 1999. Chlorophyll a fluorescence induction. *Biochimica et Biophysica Acta* **1412,** 1–28.

Lee AI, Thornber JP. 1995. Analysis of the pigment stoichiometry of pigment–protein complexes from barley (*Hordeum vulgare*). The xanthophyll cycle intermediates occur mainly in the light-harvesting complexes of photosystem I and photosystem II. *Plant Physiology* **107,** 565–574.

Lee J-E, Frankenberg C, van der Tol C, *et al*. 2013. Forest productivity and water stress in Amazonia: observations from GOSAT chlorophyll fluorescence. *Proceedings of the Royal Society B: Biological Sciences* **280,** 20130171.

Lichtenthaler HK, Rinderle U. 1988. The role of chlorophyll fluorescence in the detection of stress conditions in plants. *CRC Critical Reviews in Analytical Chemistry* **19,** S29–S85.

Liu Z, Yan H, Wang K, Kuang T, Zhang J, Gui L, An X, Chang W. 2004. Crystal structure of spinach major light-harvesting complex at 2.72 Å resolution. *Nature* **428,** 287–292.

Logan BA, Adams III WW, Demmig-Adams B. 2007. Avoiding common pitfalls of chlorophyll fluorescence analysis under field conditions. *Functional Plant Biology* **34,** 853–859.

Long SP, Bernacchi CJ. 2003. Gas exchange measurements, what can they tell us about the underlying limitations to photosynthesis? Procedures and sources of error. *Journal of Experimental Botany* **54,** 2393–2401.

Lu C, Lu Q, Zhang J, Kuang T. 2001. Characterization of photosynthetic pigment composition, photosystem II photochemistry and thermal energy dissipation during leaf senescence of wheat plants grown in the field. *Journal of Experimental Botany* **52,** 1805–1810.

Malenovský Z, Mishra KB, Zemek F, Rascher U, Nedbal L. 2009. Scientific and technical challenges in remote sensing of plant canopy reflectance and fluorescence. *Journal of Experimental Botany* **60,** 2987–3004.

Martin B, Mårtensson O, Öquist G. 1978. Seasonal effects on photosynthetic electron transport and fluorescence properties in isolated chloroplasts of *Pinus sylvestris*. *Physiologia Plantarum* **44,** 102–109.

Matsubara S, Chow WS. 2004. Populations of photoinactivated photosystem II reaction centers characterized by chlorophyll a fluorescence lifetime *in vivo*. *Proceedings of the National Academy of Sciences, USA* **101,** 18234–18239.

Maxwell K, Johnson GN. 2000. Chlorophyll fluorescence—a practical guide. *Journal of Experimental Botany* **51,** 659–668.

Mehta P, Allakhverdiev SI, Jajoo A. 2010. Characterization of photosystem II heterogeneity in response to high salt stress in wheat leaves (*Triticum aestivum*). *Photosynthesis Research* **105,** 249–255.

Melis A. 1991. Dynamics of photosynthetic membrane composition and function. *Biochimica et Biophysica Acta* **1058,** 87–106.

Meroni M, Rossini M, Guanter L, Alonso L, Rascher U, Colombo R, Moreno J. 2009. Remote sensing of solar-induced chlorophyll fluorescence: review of methods and applications. *Remote Sensing of Environment* **113,** 2037–2051.

Merzlyak MN, Chivkunova OB, Solovchenko AE, Naqvi KR. 2008. Light absorption by anthocyanins in juvenile, stressed, and senescing leaves. *Journal of Experimental Botany* **59,** 3903–3911.

Miller J, Berger M, Goulas Y, *et al.* 2005. *Development of vegetation fluorescence canopy model*. ESTEC Contract No. 16365/02/NL/FF, Final Report.

Miloslavina Y, Szczepaniak M, Müller M, Sander J, Nowaczyk M, Rögner M, Holzwarth A. 2006. Charge separation kinetics in intact photosystem II core particles is trap-limited. A picosecond fluorescence study. *Biochemistry* **45,** 2436–2442.

Monteith JL. 1972. Solar radiation and productivity in tropical ecosystems. *Journal of Applied Ecology* **9,** 747–766.

Mooney HA, Ehleringer J, Björkman O. 1977. The energy balance of leaves of the evergreen desert shrub *Atriplex hymenelytra*. *Oecologia* **29,** 301–310.

Morales F, Abadía A, Abadía J, Montserrat G, Gil-Pelegrín E. 2002. Trichomes and photosynthetic pigment composition changes: responses of *Quercus ilex* subsp. *ballota* (Desf.) Samp. and *Quercus coccifera* L. to Mediterranean stress conditions. *Trees* **16,** 504–510.

Moreno J, Asner GP, Bach H, *et al.* 2006. Fluorescence explorer (FLEX): an optimized payload to map vegetation photosynthesis from space. In: *AIAA 57th International Astronautical Congress* , Vol, **3**. Valencia: IAC, 2065–2074.

Morton DC, Nagol J, Carabajal CC, Rosette J, Palace M, Cook BD, Vermote EF, Harding DJ, North PR. 2014. Amazon forests maintain consistent canopy structure and greenness during the dry season. *Nature* **506,** 221–224.

Moya I, Camenen L, Evain S, Goulas Y, Cerovic ZG, Latouche G, Flexas J, Ounis A. 2004. A new instrument for passive remote sensing: 1. Measurements of sunlight-induced chlorophyll fluorescence. *Remote Sensing of Environment* **91,** 186–197.

Müller P, Li X-P, Niyogi KK. 2001. Non-photochemical quenching. A response to excess light energy. *Plant Physiology* **125,** 1558–1566.

Murata N. 1969. Control of excitation transfer in photosynthesis. 1. Light-induced change of chlorophyll a fluorescence in *Porphyridium cruentum*. *Biochimica et Biophysica Acta* **172,** 242–251.

Nedbal L, Szöcs V. 1986. How long does excitonic motion in the photosynthetic unit remain coherent? *Journal of Theoretical Biology* **120,** 411–418.

Nichol CJ, Rascher U, Matsubara S, Osmond B. 2006. Assessing photosynthetic efficiency in an experimental mangrove canopy using remote sensing and chlorophyll fluorescence. *Trees* **20,** 9–15.

Nield J, Barber J. 2006. Refinement of the structural model for the Photosystem II supercomplex of higher plants. *Biochimica et Biophysica Acta* **1757,** 353–361.

Niinemets Ü, Kollist H, García-Plazaola JI, Hernández A, Becerril JM. 2003. Do the capacity and kinetics for modification of xanthophyll cycle pool size depend on growth irradiance in temperate trees? *Plant, Cell and Environment* **26,** 1787–1801.

Nilkens M, Kress E, Lambrev P, Miloslavina Y, Müller M, Holzwarth AR, Jahns P. 2010. Identification of a slowly inducible zeaxanthin-dependent component of non-photochemical quenching of chlorophyll fluorescence generated under steady-state conditions in *Arabidopsis*. *Biochimica et Biophysica Acta* **1797,** 466–475.

Nixon PJ. 2000. Chlororespiration. *Philosophical Transactions of the Royal Society B: Biological Sciences* **355,** 1541–1547.

Novoderezhkin VI, van Grondelle R. 2010. Physical origins and models of energy transfer in photosynthetic light-harvesting. *Physical Chemistry Chemical Physics* **12,** 7352–7365.

Ogaya R, Peñuelas J. 2003. Comparative seasonal gas exchange and chlorophyll fluorescence of two dominant woody species in a Holm Oak Forest. *Flora* **198,** 132–141.

Ögren E, Öquist G, Hällgren J-E. 1984. Photoinhibition of photosynthesis in *Lemna gibba* as induced by the interaction between light and temperature. III. Chlorophyll fluorescence at 77 K. *Physiologia Plantarum* **62,** 193–200.

Ogren WL. 1984. Photorespiration: pathways, regulation, and modification. *Annual Review of Plant Physiology* **35,** 415–442.

Ohad I, Kyle DJ, Arntzen CJ. 1984. Membrane protein damage and repair: removal and replacement of inactivated 32-kilodalton polypeptides in chloroplast membranes. *Journal of Cell Biology* **99,** 481–485.

Oja V, Laisk A. 2012. Photosystem II antennae are not energetically connected: evidence based on flash-induced O2 evolution and chlorophyll fluorescence in sunflower leaves. *Photosynthesis Research* **114,** 15–28.

Olascoaga B, Juurola E, Pinho P, Lukes P, Halonen L, Nikinmaa E, Bäck J, Porcar-Castell A. 2014. Seasonal variation in the reflectance of photosynthetically active radiation from epicuticular waxes of Scots pine (*Pinus sylvestris*) needles. *Boreal Environment Research* (in press).

Ort DR, Yocum CF, **eds.** 1996. *Oxygenic photosynthesis: the light reactions. Advances in Photosynthesis* , Vol. **4**. Dordrecht: Kluwer Academic Publishers.

Ottander C, Campbell D, Öquist G. 1995. Seasonal changes in photosystem II organisation and pigment composition in Pinus sylvestris. *Planta* **197,** 176–183.

Ottander C, Öquist G. 1991. Recovery of photosynthesis in winter-stressed Scots pine. *Plant, Cell and Environment* **14,** 345–349.

Owens TG, Shreve AP, Albert AC. 1992. Dynamics and mechanisms of singlet energy transfer between carotenoids and chlorophylls: light harvesting and non-photochemical fluorescence quenching. In: Murata N, ed. *Research in photosynthesis* , Vol. **I**. Dordrecht: Kluwer Academic Publishers, 179–186.

Palombi L, Cecchi G, Lognoli D, Raimondi V, Toci G, Agati G. 2011. A retrieval algorithm to evaluate the Photosystem I and Photosystem II spectral contributions to leaf chlorophyll fluorescence at physiological temperatures. *Photosynthesis Research* **108,** 225–239.

Pedrós R, Goulas Y, Jacquemoud S, Louis J, Moya I. 2010. FluorMODleaf: a new leaf fluorescence emission model based on the PROSPECT model. *Remote Sensing of Environment* **114,** 155–167.

Pedrós R, Moya I, Goulas Y, Jacquemoud S. 2008. Chlorophyll fluorescence emission spectrum inside a leaf. *Photochemical and Photobiological Sciences* **7,** 498–502.

Peterson RB, Oja V, Laisk A. 2001. Chlorophyll fluorescence at 680 and 730 nm and leaf photosynthesis. *Photosynthesis Research* **70,** 185–196.

Pfannschmidt T, Nilsson A, Allen JF. 1999. Photosynthetic control of chloroplast gene expression. *Nature* **397,** 625–628.

Pfündel E. 1998. Estimating the contribution of photosystem I to total leaf chlorophyll fluorescence. *Photosynthesis Research* **56,** 185–195.

Pfündel EE. 2009. Deriving room temperature excitation spectra for photosystem I and photosystem II fluorescence in intact leaves from the dependence of F V/F M on excitation wavelength. *Photosynthesis Research* **100,** 163–177.

Pfündel EE, Agati G, Cerovic ZG. 2006. Optical properties of plant surfaces. In: Riederer M, Muller C, eds. *Biology of the plant cuticle. Annual Plant Reviews* , Vol. **23**. Oxford: Blackwell Publishing, 216–249.

Pfündel EE, Klughammer C, Meister A, Cerovic ZG. 2013. Deriving fluorometer-specific values of relative PSI fluorescence intensity from quenching of F0 fluorescence in leaves of Arabidopsis thaliana and Zea mays. *Photosynthesis Research* **113,** 189–206.

Pieruschka R, Klimov D, Kolber ZS, Berry JA. 2010. Monitoring of cold and light stress impact on photosynthesis by using the laser induced fluorescence transient (LIFT) approach. *Functional Plant Biology* **37,** 395–402.

Plascyk JA. 1975. The MkII Fraunhofer line discriminator (FLD-II) for airborne and orbital remote sensing of solar-stimulated luminescence. *Optical Engineering* **14,** 339–330.

Porcar-Castell A. 2011. A high-resolution portrait of the annual dynamics of photochemical and non-photochemical quenching in needles of Pinus sylvestris. *Physiologia Plantarum* **143,** 139–153.

Porcar-Castell A, Bäck J, Juurola E, Hari P. 2006. Dynamics of the energy flow through photosystem II under changing light conditions: a model approach. *Functional Plant Biology* **33,** 229–239.

Porcar-Castell A, Garcia-Plazaola JI, Nichol CJ, Kolari P, Olascoaga B, Kuusinen N, Fernández-Marín B, Pulkkinen M, Juurola E, Nikinmaa E. 2012. Physiology of the seasonal relationship between the photochemical reflectance index and photosynthetic light use efficiency. *Oecologia* **170,** 313–323.

Porcar-Castell A, Juurola E, Ensminger I, Berninger F, Hari P, Nikinmaa E. 2008*a*. Seasonal acclimation of photosystem II in Pinus sylvestris. II. Using the rate constants of sustained thermal energy dissipation and photochemistry to study the effect of the light environment. *Tree Physiology* **28,** 1483–1491.

Porcar-Castell A, Juurola E, Nikinmaa E, Berninger F, Ensminger I, Hari P. 2008*b*. Seasonal acclimation of photosystem II in Pinus sylvestris. I. Estimating the rate constants of sustained thermal energy dissipation and photochemistry. *Tree Physiology* **28,** 1475–1482.

Porcar-Castell A, Pfündel E, Korhonen JFJ, Juurola E. 2008*c*. A new monitoring PAM fluorometer (MONI-PAM) to study the short- and long-term acclimation of photosystem II in field conditions. *PhotosynthesisResearch* **96,** 173–179.

Pospíšil P, Skotnica J, Nauš J. 1998. Low and high temperature dependence of minimum F_0 and maximum F_M chlorophyll fluorescence *in vivo*. *Biochimica et Biophysica Acta* **1363,** 95–99.

Qi J, Chehbouni A, Huete AR, Kerr YH, Sorooshian S. 1994. A modified soil adjusted vegetation index. *Remote Sensing of Environment* **48,** 119–126.

Rappaport F, Béal D, Joliot A, Joliot P. 2007. On the advantages of using green light to study fluorescence yield changes in leaves. *Biochimica et Biophysica Acta* **1767,** 56–65.

Rascher U, Agati G, Alonso L, *et al*. 2009. CEFLES2: the remote sensing component to quantify photosynthetic efficiency from the leaf to the region by measuring sun-induced fluorescence in the oxygen absorption bands. *Biogeosciences Discussions* **6,** 1181–1198.

Richardson AD, Berlyn GP. 2002. Changes in foliar spectral reflectance and chlorophyll fluorescence of four temperate species following branch cutting. *Tree Physiology* **22,** 499–506.

Rintamäki E, Salonen M, Suoranta U-M, Carlberg I, Andersson B, Aro E-M. 1997. Phosphorylation of light-harvesting complex II and photosystem II core proteins shows different irradiance-dependent regulation *in vivo*. *Journal of Biological Chemistry* **272,** 30476–30482.

Rivadossi A, Zucchelli G, Garlaschi FM, Jennings RC. 1999. The importance of PS I chlorophyll red forms in light-harvesting by leaves. *Photosynthesis Research* **60,** 209–215.

Roelofs TA, Lee C, Holzwarth AR. 1992. Global target analysis of picosecond chlorophyll fluorescence kinetics from pea chloroplasts: a new approach to the characterization of the primary processes in photosystem II α- and β-units. *Biophysical Journal* **61,** 1147–1163.

Rohácek K. 2002. Chlorophyll fluorescence parameters: the definitions, photosynthetic meaning, and mutual relationships. *Photosynthetica* **40,** 13–29.

Rosema A, Snel JFH, Zahn H, Buurmeijer WF, van Hove LWA. 1998. The relation between laser-induced chlorophyll fluorescence and photosynthesis. *Remote Sensing of Environment* **65,** 143–154.

Rossini M, Meroni M, Migliavacca M, Manca G, Cogliati S, Busetto L, Picchi V, Cescatti A, Seufert G, Colombo R. 2010. High resolution field spectroscopy measurements for estimating gross ecosystem production in a rice field. *Agricultural and Forest Meteorology* **150,** 1283–1296.

Rouse JW Jr, Haas RH, Schell JA, Deering DW. 1974. Monitoring vegetation systems in the Great Plains with ERTS. In: Stanley CF, Mercanti EP, Becker MA, eds. *Third Earth resources technology satellite-1 Symposium—Volume I: technical presentations*. NASA special publication **351,** 309.

Rumeau D, Peltier G, Cournac L. 2007. Chlororespiration and cyclic electron flow around PSI during photosynthesis and plant stress response. *Plant, Cell and Environment* **30,** 1041–1051.

Ryu Y, Baldocchi DD, Kobayashi H, Ingen C, Li J, Black TA, Beringer J, Gorsel E, Knohl A, Law BE, Roupsard O. 2011. Integration of MODIS land and atmosphere products with a coupled-process model to estimate gross primary productivity and evapotranspiration from 1 km to global scales. *Global Biogeochemical Cycles* **25,** GB4017.

Santabarbara S, Agostini G, Casazza AP, Syme CD, Heathcote P, Böhles F, Evans MC, Jennings RC, Carbonera D. 2007. Chlorophyll triplet states associated with Photosystem I and Photosystem II in thylakoids of the green alga *Chlamydomonas reinhardtii*. *Biochimica et Biophysica Acta* **1767,** 88–105.

Sarvikas P, Hakala-Yatkin M, Dönmez S, Tyystjärvi E. 2010. Short flashes and continuous light have similar photoinhibitory efficiency in intact leaves. *Journal of Experimental Botany* **61,** 4239–4247.

Schatz GH, Brock H, Holzwarth AR. 1988. Kinetic and energetic model for the primary processes in photosystem II. *Biophysical Journal* **54,** 397–405.

Schreiber U, Schliwa U, Bilger W. 1986. Continuous recording of photochemical and non-photochemical chlorophyll fluorescence quenching with a new type of modulation fluorometer. *Photosynthesis Research* **10,** 51–62.

Schreiber U. 2004. Pulse-amplitude-modulation (PAM) fluorometry and saturation pulse method: an overview. In: Papageorgiou GC, Govindjee, eds. *Chlorophyll a fluorescence, a signature of photosynthesis. Advances*

in Photosynthesis and Respiration , Vol. **19**. Dordrecht: Springer, 279–319.

Sellers PJ. 1985. Canopy reflectance, photosynthesis and transpiration. *International Journal of Remote Sensing* **6,** 1335–1372.

Shinkarev VP, Govindjee. 1993. Insight into the relationship of chlorophyll a fluorescence yield to the concentration of its natural quenchers in oxygenic photosynthesis. *Proceedings of the National Academy of Sciences, USA* **90,** 7466–7469.

Sims DA, Luo H, Hastings S, Oechel WC, Rahman AF, Gamon JA. 2006. Parallel adjustments in vegetation greenness and ecosystem CO_2 exchange in response to drought in a Southern California chaparral ecosystem. *Remote Sensing of Environment* **103,** 289–303.

Sonoike K. 2011. Photoinhibition of photosystem I. *Physiologia Plantarum* **142,** 56–64.

Soukupová J, Cséfalvay L, Urban O, Košvancová M, Marek M, Rascher U, Nedbal L. 2008. Annual variation of the steady-state chlorophyll fluorescence emission of evergreen plants in temperate zone. *Functional Plant Biology* **35,** 63–76.

Stirbet A. 2013. Excitonic connectivity between photosystem II units: what is it, and how to measure it? *Photosynthesis Research* **116,** 189–214.

Strand M, Lundmark T. 1987. Effects of low night temperature and light on chlorophyll fluorescence of field-grown seedlings of Scots pine (*Pinus sylvestris* L.). *Tree Physiology* **3,** 211–224.

Stylinski CD, Gamon JA, Oechel WC. 2002. Seasonal patterns of reflectance indices, carotenoid pigments and photosynthesis of evergreen chaparral species. *Oecologia* **131,** 366–374.

Tan X, Xu D, Shen Y. 1998. Both spillover and light absorption cross-section changes are involved in the regulation of excitation energy distribution between the two photosystems during state transitions in wheat leaf. *Photosynthesis Research* **56,** 95–102.

Thayer SS, Björkman O. 1992. Carotenoid distribution and deepoxidation in thylakoid pigment–protein complexes from cotton leaves and bundle-sheath cells of maize. *Photosynthesis Research* **33,** 213–225.

Tikkanen M, Grieco M, Aro E-M. 2011. Novel insights into plant light-harvesting complex II phosphorylation and 'state transitions'. *Trends in Plant Science* **16,** 126–131.

Trissl H-W, Wilhelm C. 1993. Why do thylakoid membranes from higher plants form grana stacks? *Trends in Biochemical Sciences* **18,** 415–419.

Tyystjärvi E. 2004. Phototoxicity. In: Noodén LD, ed. *Plant cell death processes*. San Diego: Academic Press, 271–283.

Tyystjarvi E. 2013. Photoinhibition of Photosystem II. *International Review of Cell and Molecular Biology* **300,** 243–303.

Tyystjarvi E, Aro E-M. 1996. The rate constant of photoinhibition, measured in lincomycin-treated leaves, is directly proportional to light intensity. *Proceedings of the National Academy of Sciences, USA* **93,** 2213–2218.

Tyystjärvi E, Rantamäki S, Tyystjärvi J. 2009. Connectivity of photosystem II is the physical basis of retrapping in photosynthetic thermoluminescence. *Biophysical Journal* **96,** 3735–3743.

van der Tol C, Verhoef W, Timmermans J, Verhoef A, Su Z. 2009. An integrated model of soil–canopy spectral radiances, photosynthesis, fluorescence, temperature and energy balance. *Biogeosciences* **6,** 3109–3129.

van Grondelle R, Novoderezhkin VI. 2006. Energy transfer in photosynthesis: experimental insights and quantitative models. *Physical Chemistry Chemical Physics* **8,** 793–807.

van Kooten O, Snel JF. 1990. The use of chlorophyll fluorescence nomenclature in plant stress physiology. *Photosynthesis Research* **25,** 147–150.

Vassiliev S, Bruce D. 2008. Toward understanding molecular mechanisms of light harvesting and charge separation in photosystem II. *Photosynthesis Research* **97,** 75–89.

Verhoef W. 1984. Light scattering by leaf layers with application to canopy reflectance modeling: the SAIL model. *Remote Sensing of Environment* **16,** 125–141.

Verhoeven A. 2014. Sustained energy dissipation in winter evergreens. *New Phytologist* **201,** 57–65.

Verhoeven AS, Adams WW III, Demmig-Adams B. 1996. Close relationship between the state of the xanthophyll cycle pigments and photosystem II efficiency during recovery from winter stress. *Physiologia Plantarum* **96,** 567–576.

Vernotte C, Etienne AL, Briantais JM. 1979. Quenching of the system II chlorophyll fluorescence by the plastoquinone pool. *Biochimica et Biophysica Acta* **545,** 519–527.

Vogelmann TC. 1993. Plant tissue optics. *Annual Review of Plant Biology* **44,** 231–251.

Vogelmann TC, Evans JR. 2002. Profiles of light absorption and chlorophyll within spinach leaves from chlorophyll fluorescence. *Plant, Cell and Environment* **25,** 1313–1323.

Walters RG. 2005. Towards an understanding of photosynthetic acclimation. *Journal of Experimental Botany* **56,** 435–447.

Weis E, Berry JA. 1987. Quantum efficiency of photosystem II in relation to 'energy'-dependent quenching of chlorophyll fluorescence. *Biochimica et Biophysica Acta* **894,** 198–208.

Weis E, Berry JA. 1988. Plants and high temperature stress. In: Long SP, Woodward FI, eds. *Plants and temperature. Symposium No 42*. Cambridge: Society of Experimental Biology, 329–346.

Williams M, Richardson AD, Reichstein M, ***et al***. 2009. Improving land surface models with FLUXNET data. *Biogeosciences* **6,** 1341–1359.

Xiao X, Zhang Q, Braswell B, Urbanski S, Boles S, Wofsy S, Moore B III, Ojima D. 2004. Modeling gross primary production of temperate deciduous broadleaf forest using satellite images and climate data. *Remote Sensing of Environment* **91,** 256–270.

Yu F, Berg VS. 1994. Control of paraheliotropism in two *Phaseolus* species. *Plant Physiology* **106,** 1567–1573.

Zarco-Tejada PJ, Berni JA, Suárez L, Sepulcre-Cantó G, Morales F, Miller J. 2009. Imaging chlorophyll fluorescence with an airborne narrow-band multispectral camera for vegetation stress detection. *Remote Sensing of Environment* **113,** 1262–1275.

Zarco-Tejada PJ, Catalina A, González M, Martín P. 2013. Relationships between net photosynthesis and steady-state chlorophyll fluorescence retrieved from airborne hyperspectral imagery. *Remote Sensing of Environment* **136,** 247–258.

Zarco-Tejada PJ, González-Dugo V, Berni JA. 2012. Fluorescence, temperature and narrow-band indices acquired from a UAV platform for water stress detection using a micro-hyperspectral imager and a thermal camera. *Remote Sensing of Environment* **117,** 322–337.

Zarco-Tejada PJ, Miller JR, Mohammed GH, Noland TL. 2000. Chlorophyll fluorescence effects on vegetation apparent reflectance: I. Leaf-level measurements and model simulation. *Remote Sensing of Environment* **74,** 582–595.

Zarter CR, Adams WW III, Ebbert V, Adamska I, Jansson S, Demmig-Adams B. 2006. Winter acclimation of PsbS and related proteins in the evergreen *Arctostaphylos uva-ursi* as influenced by altitude and light environment. *Plant, Cell and Environment* **29,** 869–878.

Zhao M, Running S, Heinsch FA, Nemani R. 2011. MODIS-derived terrestrial primary production. In: Ramachandran B, Justice CO, Abrams MJ, eds. *Land remote sensing and global environmental change*. New York: Springer, 635–660.

Zhu X-G, Govindjee, Baker NR, deSturler E, Ort DR, Long SP. 2005. Chlorophyll a fluorescence induction kinetics in leaves predicted from a model describing each discrete step of excitation energy and electron transfer associated with Photosystem II. *Planta* **223,** 114–133.